In-depth characterization of denitrifier communities across different soil ecosystems in the tundra

Igor S. Pessi[1,2], Sirja Viitamäki[1], Anna-Maria Virkkala[3,4], Eeva Eronen-Rasimus[1,5], Tom O. Delmont[6], Maija E. Marushchak[7,8], Miska Luoto[3], and Jenni Hultman[1,2,9,*]

[1]Department of Microbiology, University of Helsinki, Helsinki, Finland; [2]Helsinki Institute of Sustainability Science (HELSUS), Helsinki, Finland; [3]Department of Geosciences and Geography, University of Helsinki, Helsinki, Finland; [4]Woodwell Climate Research Center, Falmouth, MA, USA; [5]Marine Research Centre, Finnish Environment Institute (SYKE), Helsinki, Finland; [6]Department of Bioinformatics, Genoscope, Paris, France; [7]Department of Biological and Environmental Science, University of Jyväskylä, Jyväskylä, Finland; [8]Department of Environmental and Biological Sciences, University of Eastern Finland, Kuopio, Finland; [9]Natural Resources Institute Finland (Luke), Helsinki, Finland. *Corresponding author: jenni.hultman@helsinki.fi

Abstract

Background: In contrast to earlier assumptions, there is now mounting evidence for the role of tundra soils as important sources of the greenhouse gas nitrous oxide (N_2O). However, the microorganisms involved in the cycling of N_2O in this system remain largely uncharacterized. Since tundra soils are variable sources and sinks of N_2O, we aimed at investigating differences in community structure across different soil ecosystems in the tundra. **Results:** We analysed 1.4 Tb of metagenomic data from soils in northern Finland covering a range of ecosystems from dry upland soils to water-logged fens and obtained 796 manually binned and curated metagenome-assembled genomes (MAGs). We then searched for MAGs harbouring genes involved in denitrification, an important process driving N_2O emissions. Communities of potential denitrifiers were dominated by microorganisms with truncated denitrification pathways (i.e., lacking one or more denitrification genes) and differed across soil ecosystems. Upland soils showed a strong N_2O sink potential and were dominated by members of the Alphaproteobacteria such as *Bradyrhizobium* and *Reyranella*. Fens, which had in general net-zero N_2O fluxes, had a high abundance of poorly characterized taxa affiliated with the Chloroflexota lineage Ellin6529 and the Acidobacteriota subdivision Gp23. **Conclusions:** By coupling an in-depth characterization of microbial communities with *in situ* measurements of N_2O fluxes, our results suggest that the observed spatial patterns of N_2O fluxes in the tundra are related to differences in the composition of denitrifier communities.

Keywords: Arctic; denitrification; genome-resolved metagenomics; nitrous oxide

Background

Nitrous oxide (N_2O) is a greenhouse gas (GHG) that has approximately 300 times the global warming potential of carbon dioxide on a 100-year scale [1]. Atmospheric N_2O concentrations have increased by nearly 20% since pre-industrial times, with soils – both natural and anthropogenic – accounting for up to 70% of the global emissions [2]. Despite being nitrogen (N) limited and enduring low temperatures throughout most of the year, tundra soils are increasingly recognized as important sources of N_2O [3–7]. The relative contribution of tundra soils to global GHG emissions is predicted to increase in the future [8, 9], as the warming rate at high latitude environments is more than twice as high than in other regions [10].

Microbial denitrification is an important source of N_2O [11]. Denitrification is a series of enzymatic steps in which nitrate (NO_3^-) is sequentially reduced to nitrite (NO_2^-), nitric oxide (NO), N_2O, and dinitrogen (N_2) via the activity of the Nar, Nir, Nor, and Nos enzymes, respectively. The denitrification trait is common across a wide range of archaea, bacteria, and some fungi, most of which are facultative anaerobes that switch to N oxides as electron acceptor when oxygen becomes limiting [12]. Denitrification is a modular community process performed in synergy by different microbial taxa that execute only a subset of the complete denitrification pathway [12, 13]. With the growing number of microbial genomes sequenced in recent years, it has become evident that only a fraction of the microorganisms involved in the denitrification pathway encode the enzymatic machinery needed for complete denitrification [14, 15].

Compared to high N_2O-emitting systems such as agricultural and tropical soils, our knowledge of denitrifier communities in tundra soils is limited. As denitrification leads to the loss of N to the atmosphere, it enhances the N-limited status of tundra systems thus impacting both microbial and plant communities [16, 17]. Investigations of denitrifier diversity in the tundra have been largely limited to gene-centric surveys using microarrays, amplicon sequencing, qPCR, and read-based metagenomics, which provide limited information on the taxonomic identity and genomic composition of community members. These studies have shown that denitrifier communities in the tundra are dominated by members of the phyla Proteobacteria, Actinobacteria, and Bacteroidetes, and that the potential for complete denitrification is usually present at the community level [18–22]. However, it is not known whether the complete denitrification potential occurs within discrete microbial populations or is widespread throughout populations of truncated denitrifiers lacking one or more denitrification genes. In addition, tundra soils encompass many different ecosystems, some of which are notorious N_2O sources (e.g. bare peat surfaces [3]). N_2O consumption is usually favoured in wetlands, where low NO_3^- availability due to anoxia promotes the reduction of N_2O to N_2 [23]. In upland soils,

N_2O fluxes vary in both time and space. Strong N_2O sinks have been observed specially in sparsely vegetated upland soils [7], but the microbial processes underlying N_2O consumption in these systems are largely unknown [24]. Altogether, these large differences in N_2O fluxes across tundra ecosystems indicate differences in the structure of microbial communities, but a comprehensive understanding of the microorganisms driving N_2O fluxes in tundra soils is lacking.

Modelling N_2O emissions based on microbial community structure is challenging. N_2O fluxes are characterized by a high temporal and spatial heterogeneity driven by several environmental constraints related to soil pH, N, moisture, and oxygen content [11]. In addition, our knowledge of the regulation of the denitrification process is largely based on the activity of model organisms such as the complete denitrifier *Paracoccus denitrificans* [25]. It has been suggested that incomplete denitrifiers that contain Nir and Nor but lack Nos contribute substantially to soil N_2O emissions [26], while non-denitrifying N_2O reducers, i.e. microorganisms that contain Nos but lack Nir, can represent an important N_2O sink [27–29]. Furthermore, the partitioning of metabolic pathways across different populations with truncated pathways – also known as metabolic handoffs [30] – has been linked to higher efficiencies in substrate consumption compared to complete pathways [15, 31]. However, it remains largely unclear how populations of truncated denitrifiers with different sets of denitrification genes interact with each other and the environment impacting *in situ* N_2O emissions.

The paucity of in-depth knowledge on denitrifying communities in the tundra impairs our ability to model current and future N_2O fluxes from this biome. A better understanding of the ecological, metabolic, and functional traits of denitrifiers is thus critical for improving current models and mitigating N_2O emissions [32]. This invariably relies on the characterization of the so-called uncultured majority, i.e. microorganisms that have not been cultured to date but which comprise a high proportion of the microbial diversity in complex ecosystems [33, 34]. Genome-resolved metagenomics is a powerful tool to access the genomes of uncultured microorganisms and has provided important insights into carbon cycling processes in tundra soils [35–37]. However, this approach has not yet been applied to investigate the mechanisms driving N_2O fluxes in the tundra. Here, we used genome-resolved metagenomics to investigate the diversity and metabolic capabilities of denitrifiers across different tundra soil ecosystems characterised by a high variability in net N_2O fluxes in an area of mountain tundra in Kilpisjärvi, northern Finland.

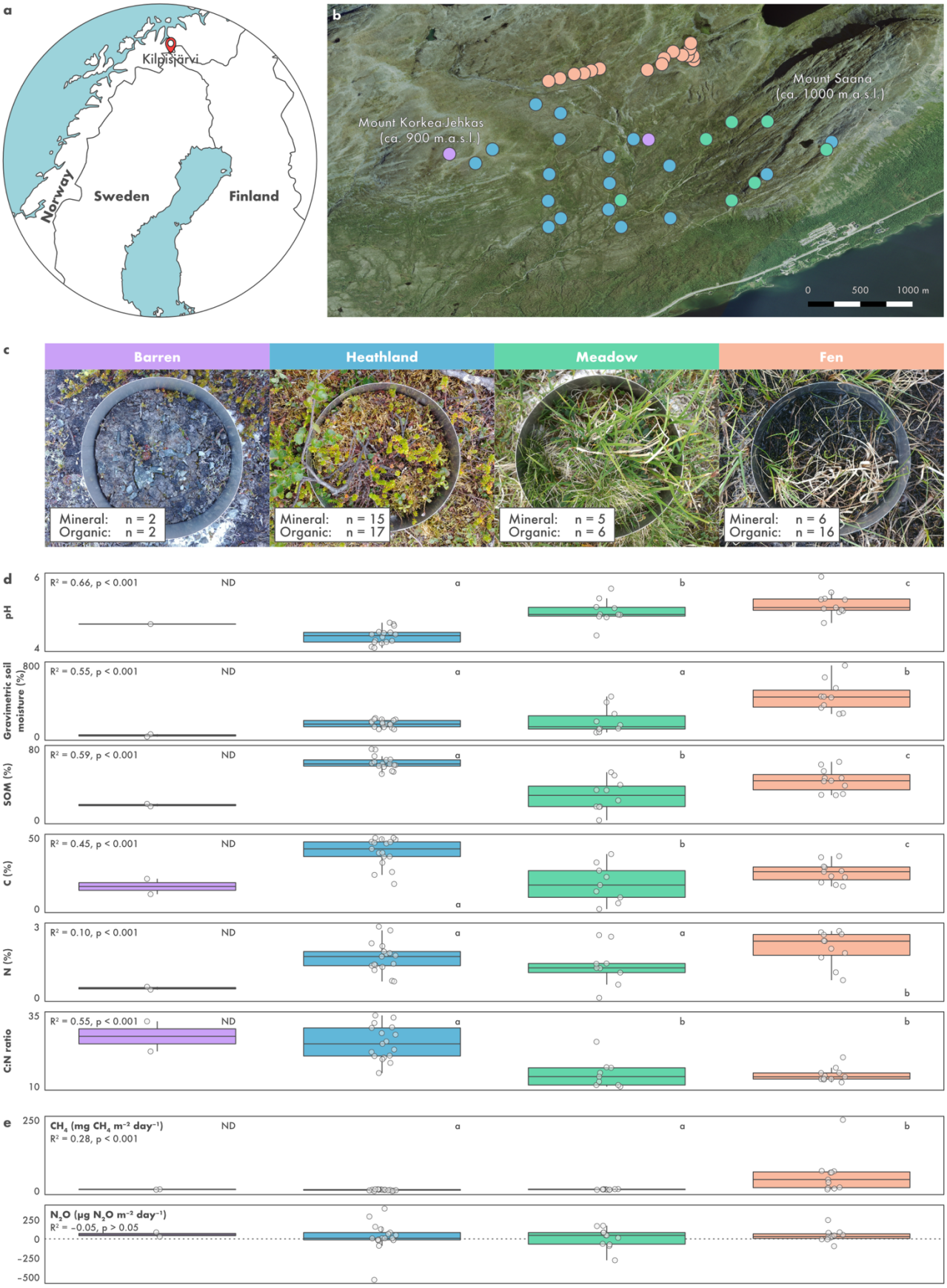
a
Kilpisjärvi
Norway
Sweden
Finland
b
Mount Korkea-Jehkas
(ca. 900 m.a.s.l.)
Mount Saana
(ca. 1000 m.a.s.l.)
0
500
1000 m
c
Barren
Heathland
Meadow
Fen
Mineral: n = 2
Organic: n = 2
Mineral: n = 15
Organic: n = 17
Mineral: n = 5
Organic: n = 6
Mineral: n = 6
Organic: n = 16
d
pH
Gravimetric soil moisture (%)
SOM (%)
C (%)
N (%)
C:N ratio
R² = 0.66, p < 0.001
R² = 0.55, p < 0.001
R² = 0.59, p < 0.001
R² = 0.45, p < 0.001
R² = 0.10, p < 0.001
R² = 0.55, p < 0.001
ND
e
CH4 (mg CH4 m⁻² day⁻¹)
R² = 0.28, p < 0.001
N2O (µg N2O m⁻² day⁻¹)
R² = −0.05, p > 0.05

(Previous page) Fig. 1 | Saana Nature Reserve, an area of mountain tundra in Kilpisjärvi, northern Finland. a) Map of Fennoscandia showing the location of Kilpisjärvi. **b)** Aerial overview of the study area showing the location of the 43 sites sampled for metagenomic analysis. Image provided by the National Land Survey of Finland under the Creative Commons CC BY 4.0 license. **c)** *In situ* photographs of the four types of soil ecosystems investigated. **d)** Physicochemical characterization of the soil ecosystems based on 41 organic and 28 mineral samples taken from the 43 sites. **e)** *In situ* ecosystem-level nitrous oxide (N_2O) and methane (CH_4) fluxes measured from the 43 sites using a static, non-steady state, non-flow-through system. Negative values represent net uptake and positive net emissions. For clarity, one outlier measurement from a meadow site (660 μg N_2O m^{-2} day^{-1}) was removed. In panels d and e, ecosystems followed by different letters are significantly different (one-way ANOVA, $p < 0.05$). Samples from barren soils were not included in the ANOVA procedure due to the limited number of samples (ND: not determined).

Methods

Study area and sampling

The Saana Nature Reserve (69.04°N, 20.79°E) is located in Kilpisjärvi, northern Finland **(Fig. 1a)**. The area is part of the mountain tundra biome and is characterized by a mean annual temperature of –1.9°C and annual precipitation of 487 mm [38]. Our study sites are distributed across Mount Saana and Mount Korkea-Jehkas and the valley in between **(Fig. 1b)**, and include barren soils, heathlands (dominated by evergreen and deciduous shrubs), meadows (dominated by graminoids and forbs), and fens **(Fig. 1c)**. Sampling was performed across 43 sites (barren soils, n = 2; heathlands, n = 18; meadows, n = 7; fens, n = 16) during the peak of the growing season in the northern hemisphere. Fen sites were sampled in July 2018 and all other sites in July 2017. Samples were obtained with a soil corer sterilized with 70% ethanol and, when possible, cores were split into organic and mineral samples using a sterilized spatula. In total, 69 samples (41 organic and 28 mineral) were obtained from the 43 sites **(Figure 1c, Suppl. Table S1)**. Samples were transferred to a whirl-pack bag and immediately frozen in dry ice. Samples were transported frozen to the laboratory at the University of Helsinki and kept at –80°C until analyses.

Soil physicochemical characterization and *in situ* measurement of GHG fluxes

Soil pH, moisture, and soil organic matter (SOM) content were measured from the 69 samples according to Finnish (SFS) and international (ISO) standards (SFS 300, ISO 10390, and SFS

131 3008). Carbon (C) and N content were measured using a Vario Micro Cube machine (Elementar,
132 Langenselbold, Germany). *In situ* ecosystem-level N_2O and methane (CH_4) fluxes were
133 measured from the 43 sites using a static, non-steady state, non-flow-through system composed
134 of a darkened acrylic chamber (20 cm diameter, 25 cm height) [4, 39]. Measurements were
135 conducted between 2nd July and 2nd August 2018, between 10 am and 5 pm. Simultaneous
136 measurement of GHG fluxes and sampling for metagenomic sequencing was not possible due to
137 limited resources and logistic constraints. At each site, five 25 mL gas samples were taken
138 during a 50-minute chamber closure and transferred to evacuated Exetainer vials (Labco,
139 Lampeter, UK). Gas samples were analysed using an Agilent 7890B gas chromatograph (Agilent
140 Technologies, Santa Clara, CA, USA) equipped with an autosampler (Gilson, Middleton, WI,
141 USA) and a flame ionization detector for CH_4 and an electron capture detector for N_2O. Gas
142 concentrations were calculated from the gas chromatograph peak areas based on standard
143 curves with a CH_4 concentration of 0–100 ppm and a N_2O concentration of 0–5000 ppb.
144 Differences in physicochemical composition and rates of GHG fluxes across soil ecosystems were
145 assessed using one-way analysis of variance (ANOVA) followed by Tukey's HSD test with the
146 *lm* and *TukeyHSD* functions in R v3.6.3 (https://www.r-project.org). Due to the limited number
147 of samples from barren sites, these were not included in the ANOVA procedure.

148 **Metagenome sequencing and processing of raw data**

149 Total DNA and RNA were co-extracted as previously described [40]. Briefly, extraction was
150 performed on 0.5 g of soil using a hexadecyltrimethyl ammonium bromide (CTAB), phenol-
151 chloroform, and bead-beating protocol. DNA was purified using the AllPrep DNA Mini Kit
152 (QIAGEN, Hilden, Germany) and quantified using the Qubit dsDNA BR Assay Kit
153 (ThermoFisher Scientific, Waltham, MA, USA). Library preparation for Illumina metagenome
154 sequencing was performed using the Nextera XT DNA Library Preparation Kit (Illumina, San
155 Diego, CA, USA). Metagenomes were obtained for 69 samples across two paired-end NextSeq
156 (132–170 bp) and one NovaSeq (2 x 151 bp) runs **(Suppl. Table S1)**. Two samples were
157 additionally sequenced with Nanopore MinION. For this, libraries were prepared using the
158 SQK-LSK109 Ligation Sequencing Kit with the long fragment buffer (Oxford Nanopore
159 Technologies, Oxford, UK) and the NEBNext Companion Module for Oxford Nanopore
160 Technologies Ligation Sequencing Kit (New England Biolabs). Each sample was sequenced for
161 48 hours on one R9.4 flow cell.

162 We obtained more than 9 billion Illumina (1.4 Tb) and 7 million Nanopore (21.5 Gb) reads from
163 the 69 soil metagenomes (mean: 19.9 Gb, minimum: 0.7 Gb, maximum: 82.9 Gb) **(Suppl. Table**
164 **S1)**. The quality of the raw Illumina data was verified with fastQC v0.11.9

165 (https://www.bioinformatics.babraham.ac.uk/projects/fastqc) and multiQC v1.8 [41]. Cutadapt
166 v1.16 [42] was then used to trim sequencing adapters and low-quality base calls (q < 20) and to
167 filter out short reads (< 50 bp). Nanopore data were basecalled with GPU guppy v4.0.11 using
168 the high-accuracy model and applying a minimum quality score of 7. The quality of the
169 basecalled Nanopore data was assessed with pycoQC v2.5.0.21 [43] and adapters were trimmed
170 with Porechop v0.2.4 (https://github.com/rrwick/Porechop).

171 **Taxonomic profiling**

172 Taxonomic profiles of the microbial communities were obtained using a read-based approach,
173 i.e., based on unassembled Illumina data. Due to differences in sequencing depth across the
174 samples, the dataset was resampled to 2,000,000 reads per sample with seqtk v1.3
175 (https://github.com/lh3/seqtk). Reads matching the SSU rRNA gene were identified with
176 METAXA v2.2 [44] and classified against the SILVA database release 138.1 [45] in mothur
177 v1.44.3 [46] using the Wang's Naïve Bayesian Classifier [47] and a 80% confidence cut-off.
178 Differences in community structure were assessed using non-metric multidimensional scaling
179 (NMDS) and permutational ANOVA (PERMANOVA) with the package vegan v2.5.6
180 (https://cran.r-project.org/web/packages/vegan) in R v3.6.3 (functions *metaMDS* and *adonis*,
181 respectively). Relationships between the abundance of individual genera and N_2O flux rates
182 were assessed using linear regression in R v3.6.3 (https://www.r-project.org).

183 **Metagenome assembling and binning**

184 Metagenome assembling of the Illumina data was performed as two co-assemblies. One co-
185 assembly comprised the upland soils (barren, heathland, and meadow; n = 47) and the other the
186 fen samples (n = 22). For each co-assembly, reads from the respective samples were pooled and
187 assembled with MEGAHIT v1.1.1.2 [48]. Assembling of the Nanopore data was done for each
188 sample individually with metaFlye v2.7.1 [49], and contigs were corrected based on Illumina
189 data from the respective sample with bowtie v2.3.5 [50], SAMtools v1.9 [51], and pilon v1.23
190 [52]. Quality assessment of the (co-)assemblies was obtained with metaQUAST v5.0.2 [53].

191 MAG binning was done separately for each Illumina and Nanopore (co-)assembly with anvi'o
192 v6.2 [54] after discarding contigs shorter than 2500 bp. The two Illumina co-assemblies and the
193 two individual Nanopore assemblies yielded more than 4 million contigs longer than 2,500 bp,
194 with a total assembly size of 21.1 Gb. Gene calls were predicted with prodigal v2.6.3 [55]. Single-
195 copy genes were identified with HMMER v.3.2.1 [56] and classified with DIAMOND v0.9.14 [57]
196 against the Genome Taxonomy Database (GTDB) release 04-RS89 [58, 59]. Illumina reads were
197 mapped to the contigs with bowtie v2.3.5 [50] and SAM files were sorted and indexed using

198 SAMtools v1.9 [51]. The co-assemblies covered a significant fraction of the original metagenomic
199 data, with an average read recruitment rate of 54.6% across samples (minimum: 22.9%,
200 maximum: 75.8%). Due to their large sizes, Illumina co-assemblies were split into 100 smaller
201 clusters based on differential coverage and tetranucleotide frequency with CONCOCT v1.0.0
202 [60]. Contigs were then manually sorted into bins based on the same composition and coverage
203 metrics using the *anvi-interactive* interface in anvi'o v6.2 [54]. Nanopore contigs were binned
204 directly without pre-clustering. Bins that were ≥ 50% complete according to the presence of
205 single-copy genes were further refined using the *anvi-refine* interface in anvi'o v6.2 [54]. In
206 addition to taxonomic signal (based on single-copy genes classified against GTDB), either
207 differential coverage or tetranucleotide frequency was used to identify and remove outlying
208 contigs. The former was used for bins with a large variation in contig coverage across samples,
209 and the latter for those with marked differences in GC content across contigs. Medium- and
210 high-quality bins (≥ 50% complete and < 10% redundant according to the MIMAG standard [61])
211 were renamed as MAGs and kept for downstream analyses.

212 Gene-centric analyses

213 Functional profiles of the microbial communities were obtained using a gene-centric approach
214 based on assembled data. For each (co-)assembly, gene calls were translated to amino acid
215 sequences and searched against the KOfam hidden Markov model (HMM) database with
216 KofamScan v1.3.0 [62]. Only matches with scores above the pre-computed family-specific
217 thresholds were kept. Genes putatively identified as denitrification genes (*nirK*, *nirS*, *norB*, and
218 *nosZ*) were submitted to further analyses to identify false positives consisting of distant
219 homologues that are not involved in denitrification. Amino acid sequences were aligned with
220 MAFFT v7.429 [63] and alignments were visualized with Unipro UGENE v38.1 [64]. Sequences
221 were then inspected for the presence of conserved residues at positions associated with the
222 binding of co-factors and active sites: *nirK*, Cu-binding and active sites [65]; *nirS*, c-heme and
223 d_1-heme binding sites [66]; *norB*, binding of the catalytic centres cyt b, b_3, and Fe_b [67]; *nosZ*:
224 binding of the Cu_Z and Cu_A centres [67]. Sequences which did not contain the correct amino acid
225 at these positions were removed. Finally, resulting amino acid sequences were aligned with
226 MAFFT v7.429 [63] along with reference sequences from the genome of cultured denitrifiers
227 [14] and a maximum-likelihood tree was computed with FastTree v2.1.11 [68] using the
228 LG+GAMMA model. Annotation of denitrification genes was also performed for previously
229 published genomes retrieved from GenBank. These included a set of 1529 MAGs obtained from
230 soils in Stordalen Mire, northern Sweden [37], and all (n = 69) genomes of Acidobacteriota
231 strains and candidate taxa (accessed on 9 October 2020).

232 The abundance of functional genes was computed based on read coverage with CoverM v0.6.1
233 [69]. For this, Illumina reads were mapped to the contigs with minimap v2.17 [70] and coverage
234 was normalized to reads per kilobase million (RPKM). Differences in functional community
235 structure were assessed using NMDS and PERMANOVA as described above for the taxonomic
236 profiles. Differences in the abundance of individual genes across soil ecosystems were assessed
237 using ANOVA followed by Tukey's HSD test with the *lm* and *TukeyHSD* functions in R v3.6.3
238 (https://www.r-project.org). Due to the limited number of samples from barren sites, these were
239 not included in the ANOVA procedure. Relationships between the abundance of denitrification
240 genes and N_2O flux rates were assessed using linear regression in R v3.6.3.

241 Phylogenomic analyses of MAGs and metabolic reconstruction

242 Phylogenetic placement of MAGs was done based on 122 archaeal and 120 bacterial single-copy
243 genes with GTDB-Tk v1.3.0 [71] and the GTDB release 05-RS95 [58, 59]. Acidobacteriota MAGs
244 containing denitrification genes were submitted to further phylogenomic analyses alongside all
245 genomes of Acidobacteriota strains and candidate taxa available on GenBank (n = 69; accessed
246 on 9 October 2020). For this, the amino acid sequence of 23 ribosomal proteins was retrieved for
247 each genome with anvi'o v6.2 [54] and aligned with MUSCLE v3.8.1551 [72]. A maximum
248 likelihood tree was then computed based on the concatenated alignments with FastTree v2.1.11
249 using the LG+GAMMA model [68]. *Escherichia coli* ATCC 11775 was used to root the tree.

250 For metabolic reconstruction, MAGs were annotated against the KOfam HMM database [62]
251 with HMMER v.3.2.1 [56] using the pre-computed score thresholds of each HMM profile. The
252 *anvi-estimate-metabolism* program in anvi'o v6.2 [54] was then used to predict the metabolic
253 capabilities of the MAGs. A metabolic pathway was considered present in MAGs containing at
254 least 75% of the genes involved in the pathway. Carbohydrate-active enzymes (CAZymes) were
255 annotated with dbCAN v.2.0 based on the dbCAN v7 HMM database [73]. Only hits with an
256 e-value $< 1 \times 10^{-14}$ and coverage > 0.35 were considered.

257 MAG dereplication and read recruitment analysis

258 Prior to read recruitment analyses, Illumina and Nanopore MAGs were dereplicated based on
259 a 99% average nucleotide identity (ANI) threshold with fastANI v1.3 [74] to remove redundancy
260 (i.e., MAGs that were recovered multiple times across the different assemblies). Read
261 recruitment analyses were then performed with CoverM v0.6.1
262 (https://github.com/wwood/CoverM). For this, Illumina reads were mapped to the set of non-
263 redundant MAGs with minimap v2.17 [70] and relative abundances were calculated as a
264 proportion of the reads mapping to each MAG.

Results

Environmental characterization and *in situ* GHG fluxes

Our sampling design in Kilpisjärvi included two soil depths across four ecosystems that are characteristic of the tundra biome (barren soils, heathlands, meadows, and fens) **(Fig. 1a–c)**. In previous studies, we have established in the area a systematic fine-scale sampling of microclimate, soil conditions, and vegetation in topographically distinct environments [40, 75, 76]. Local variation in topography and soil properties creates a mosaic of habitats characterized by contrasting ecological conditions. This makes the study setting ideal to investigate species-environment relationships and ecosystem functioning in the tundra [40, 77, 78]. Soil ecosystems differed in vegetation cover and physicochemical composition, with fens being characterized by higher pH, moisture, and N content (one-way ANOVA, $R^2 = 0.10–0.66$, $p < 0.001$) and, together with the meadows, lower C:N ratio (one-way ANOVA, $R^2 = 0.55$, $p < 0.001$) **(Fig. 1d)**.

In situ measurements showed a high sink-source variability in net N_2O fluxes across the ecosystems **(Fig. 1e)**. Although the average N_2O flux across all sites was small (net consumption of 6 µg N_2O m^{-2} day^{-1}), high N_2O emission at rates of up to 660 µg N_2O m^{-2} day^{-1} was observed at the meadow sites. Likewise, strong N_2O consumption (up to –435 µg N_2O m^{-2} day^{-1}) was observed particularly at the heathland and meadow sites. Net CH_4 emissions were observed exclusively at the fen sites **(Fig. 1e)**.

Differences in microbial community structure across soils ecosystems

Read-based analyses of unassembled SSU rRNA gene sequences showed that microbial community composition differed across the ecosystems, with fen soils harbouring contrasting microbial communities compared to the other ecosystems (PERMANOVA, $R^2 = 0.35$, $p < 0.001$) **(Suppl. Fig. S1a)**. No differences in community structure were observed between soil depths or the interaction between soil ecosystem and depth (PERMANOVA, $p > 0.05$). Among previously described (i.e., not unclassified) taxa, microbial communities in barren, heathland, and meadow soils were dominated by aerobic and facultative anaerobic heterotrophs such as *Acidipila*/*Silvibacterium*, *Bryobacter*, *Granulicella*, *Acidothermus*, *Conexibacter*, *Mycobacterium*, *Mucilaginibacter*, *Bradyrhizobium*, and *Roseiarcus* **(Suppl. Fig. S1b)**. On the other hand, fen soils were dominated by methanogenic archaea from the genera *Methanobacterium* and *Methanosaeta* and anaerobic bacteria such as *Thermoanaerobaculum*, *Desulfobacca*, and *Smithella*, but also the putative aerobic heterotroph *Candidatus* Koribacter. We did not observe a significant relationship between the abundance of individual microbial genera and N_2O flux rates (linear regression, $p > 0.05$).

298 Communities from different ecosystems also differed in their functional potential **(Suppl. Fig.**
299 **S1c).** Denitrification genes (*nirK*, *nirS*, *norB*, and *nosZ*) were in general more abundant in the
300 meadows and fens (one-way ANOVA, R^2 = 0.48–0.76, $p < 0.001$) **(Suppl. Fig. S1d)**. Fen soils,
301 which had the highest gravimetric soil water content, also had a higher abundance of genes
302 involved in sulfate reduction (*dsrA* and *dsrB*) and methanogenesis (*mcrA* and *mcrB*) (one-way
303 ANOVA, R^2 = 0.59–0.90, $p < 0.001$), indicating the prevalence of anoxic and reductive soil
304 conditions in these wet sites. We did not observe a significant relationship between N_2O flux
305 rates and neither the abundance of individual denitrification genes nor the ratio between *nosZ*
306 and *nirK*+*nirS* abundances (linear regression, $p > 0.05$). However, the ratio between *nosZ* and
307 *nirK*+*nirS* abundances was higher in the meadows (one-way ANOVA, R^2 = 0.29, $p < 0.001$)
308 **(Suppl. Fig. S1d)**, which indicates a higher potential for N_2O consumption in this ecosystem.

309 A manually curated genomic database from tundra soil metagenomes

310 Using anvi'o [54], we obtained 8,043 genomic bins and manually curated these to a set of 796
311 medium- and high-quality MAGs (≥ 50% complete and ≤ 10% redundant according to the
312 MIMAG standard [61]) **(Suppl. Fig. S2, Suppl. Table S2)**. According to estimates based on
313 domain-specific single-copy genes, the obtained MAGs were on average 65.4% complete
314 (minimum: 50.0%, maximum: 100.0%) and 2.7% redundant (minimum: 0.0%, maximum: 9.9%)
315 **(Suppl. Table S2)**. Phylogenomic analyses based on 122 archaeal and 120 bacterial single-copy
316 genes placed the MAGs across 35 bacterial and archaeal phyla according to the GTDB
317 classification [58, 59]**.** The most represented phyla were Acidobacteriota (n = 172),
318 Actinobacteriota (n = 163), Proteobacteria (Alphaproteobacteria, n = 54; Gammaproteobacteria,
319 n = 39), Chloroflexota (n = 84), and Verrucomicrobiota (n = 43) **(Suppl. Fig. S2)**. Most MAGs
320 (n = 703) belonged to genera that do not comprise formally described species, including 303
321 MAGs that were placed outside genus-level lineages currently described in GTDB and thus
322 likely represent novel genera **(Suppl. Table S2)**.

323 To investigate their distribution across the different soil ecosystems, MAGs were dereplicated
324 based on a 99% ANI threshold, yielding a set of 761 non-redundant MAGs **(Fig. 2)**. On average,
325 15.8% of the reads from each sample were recruited by the set of non-redundant MAGs
326 (minimum: 7.6%, maximum: 30.5%). In agreement with the read-based assessment, we
327 observed differences in MAG composition across the soil ecosystems, with only 50 MAGs shared
328 between the heathland, meadow, and fen soils **(Suppl. Fig. S3a)**. Fen soils harboured the
329 highest number of MAGs, with an average of 155 MAGs per sample **(Suppl. Fig. S3b)**.
330 Although barren and fen soils had similar taxonomic richness according to the read-based
331 estimates, only a small number of MAGs was detected in the barren soils (average of four MAGs

332 per sample). This is likely a result of limited sampling and sequencing of this ecosystem, which
333 consisted of four samples and a total of 7.9 Gb of metagenomic data **(Suppl. Table S1)**. The
334 number of MAGs in heathland and meadow soils was similar (average of 47 and 63 MAGs per
335 sample, respectively) **(Suppl. Fig. S3b)**. In general, barren, heathland, and meadow soils were
336 dominated by the same set of MAGs **(Suppl. Fig. S3c)**. These included members of the
337 Acidobacteriota (*Sulfotelmatobacter* and unclassified genera in the class Acidobacteriae),
338 Actinobacteriota (*Mycobacterium* and unclassified genera in the family Streptosporangiaceae),
339 and Proteobacteria (Alphaproteobacteria: *Reyranella*, *Bradyrhizobium*, and unclassified
340 Xanthobacteraceae; Gammaproteobacteria: unclassified Steroidobacteraceae). On the other
341 hand, fen soils were dominated by MAGs that were not assigned to formally described genera,
342 including lineages of Acidobacteriota (family Koribacteraceae), Actinobacteriota (family
343 Solirubrobacteraceae), Chloroflexota (class Ellin6529), Desulfobacterota (order
344 Desulfobaccales), and Halobacterota.

345 Microorganisms from tundra soils have truncated denitrification pathways

346 To gain insights into the microorganisms involved with the cycling of N_2O in tundra soils, we
347 traced the curated denitrification genes to the set of recovered MAGs. Denitrification genes were
348 found in 110 of the 796 MAGs (13.8%) **(Suppl. Table S2)**. These were affiliated with the
349 archaeal phylum Thermoproteota and many bacterial phyla such as Proteobacteria (classes
350 Gamma- and Alphaproteobacteria), Acidobacteriota, Bacteroidota, Actinobacteriota,
351 Chloroflexota, and Verrucomicrobiota **(Fig. 3a)**. However, only 17 MAGs were assigned to a
352 validly described genera **(Suppl. Table S2)**. These included members of the Acidobacteriota
353 (*Solibacter*, *Sulfotelmatobacter*, *Terracidiphilus*, and *Gaiella*), Myxococcota
354 (*Anaeromyxobacter*), Planctomycetota (*Singulisphaera*), Proteobacteria (Alphaproteobacteria:
355 *Bauldia*, *Bradyrhizobium*, *Methylocella*, and *Reyranella*; Gammaproteobacteria: *Gallionella*
356 and *Rhizobacter*), and Verrucomicrobiota (*Lacunisphaera* and *Opitutus*). On average, 1.8% of
357 the reads in each sample were recruited by all denitrifiers combined (minimum: 0.4%,
358 maximum: 6.1%). In general, denitrifiers were most abundant in the fens (1.0–6.1%) and least
359 abundant in the heathlands (0.4–2.1%).

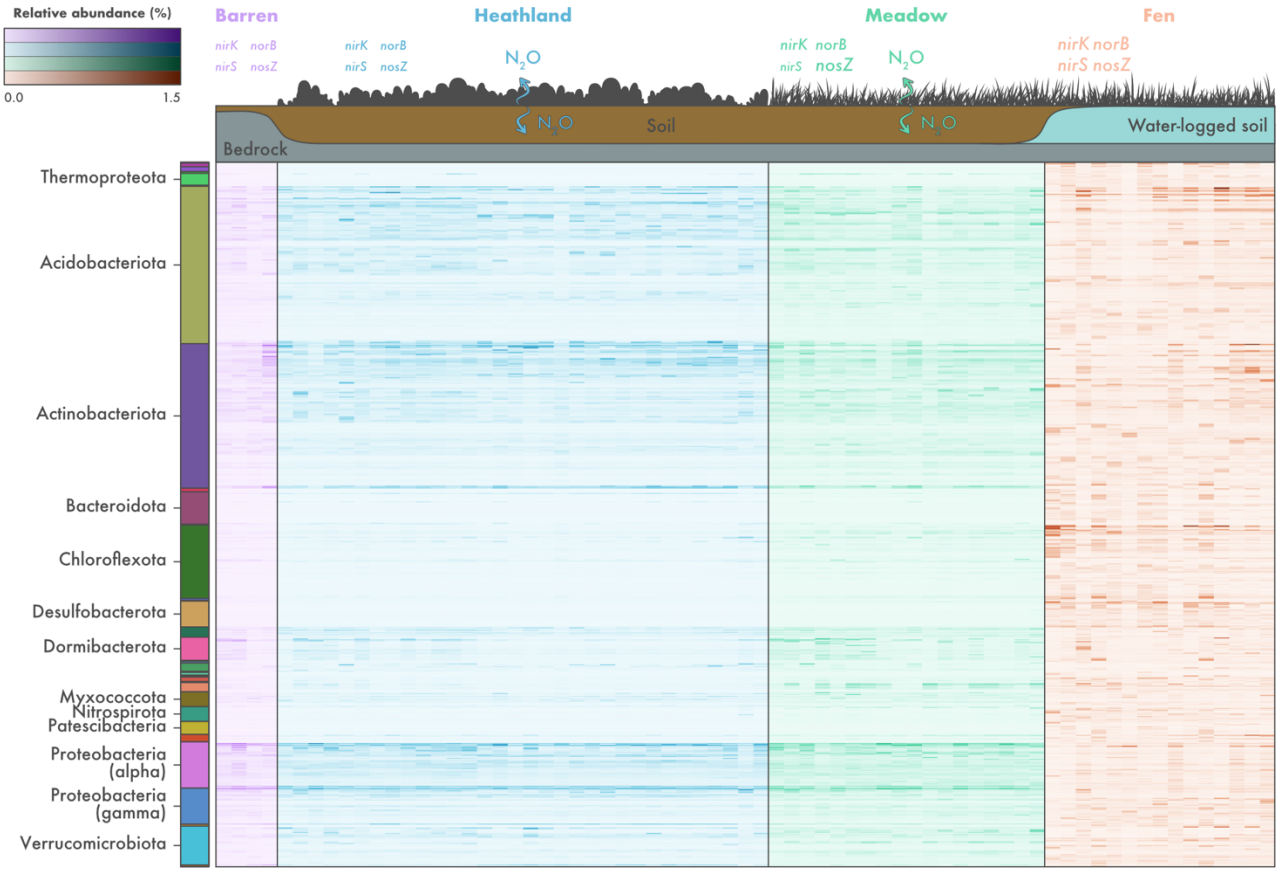

Fig. 2 | Microbial community composition across different soil ecosystems in the tundra. Relative abundance of 761 non-redundant metagenome-assembled genomes (MAGs) recovered from soils in Kilpisjärvi, northern Finland. Relative abundances were computed as a proportion of the reads mapping to each MAG. Phylum-level taxonomic assignments are shown for the major groups found. The scheme on the top of the figure represents ecosystem-level nitrous oxide (N_2O) fluxes based on *in situ* measurements **(Fig. 1)** and the abundance of denitrification genes based on a gene-centric analysis **(Suppl. Fig. S1)**. The font size of denitrification genes represents their abundance across the different ecosystems.

Genes involved in denitrification were found exclusively in MAGs with truncated denitrification pathways, i.e., MAGs missing one or more genes involved in the complete denitrification process **(Fig. 3a)**. Of the 110 MAGs harbouring denitrification genes, the vast majority (n = 104) encoded only one of the Nir, Nor, and Nos enzymes and no MAG encoded all the three enzymes required for the reduction of NO_2^- to N_2. Unsurprisingly, co-occurrence of genes encoding the three enzymes was also not observed in any of the other genomic bins of lower quality that were discarded from the final MAG dataset (i.e., bins that were < 50% complete and/or > 10% redundant). To verify if microorganisms with truncated denitrification pathways are common in other tundra systems, we expanded our analysis to 1529 MAGs recovered from permafrost

peatland, bog, and fen soils in Stordalen Mire, northern Sweden [37]. Among these, 225 MAGs (14.7%) contained denitrification genes **(Suppl. Fig. S4)**. MAGs encompassed a similar taxonomic profile as observed in the Kilpisjärvi dataset, and MAGs with truncated denitrification pathways were also the norm in Stordalen Mire soils. Only one MAG, assigned to the Gammaproteobacteria genus *Janthinobacterium*, encoded all the Nir, Nor, and Nos enzymes required for the reduction of NO_2^- to N_2.

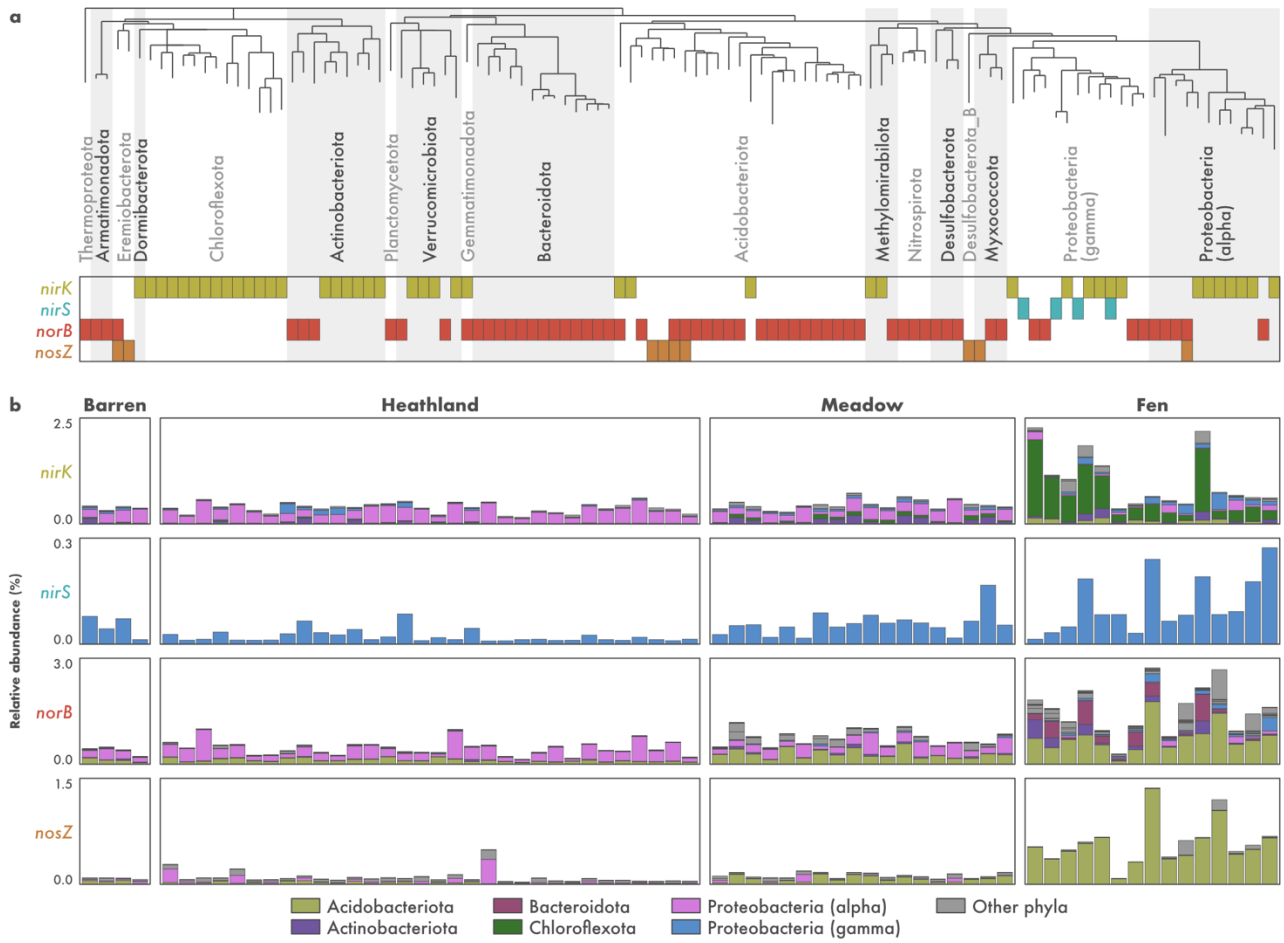

Fig. 3 | Metabolic potential for denitrification in tundra soils. a) Distribution of denitrification genes across 110 metagenome-assembled genomes (MAGs) recovered from tundra soils in Kilpisjärvi, northern Finland. Genes encoding the nitrite (*nirK*/*nirS*), nitric oxide (*norB*), and nitrous oxide (*nosZ*) reductases were annotated using a three-step approach including (1) identification using hidden Markov models from the KOfam database, (2) manual inspection for the presence of conserved residues at positions associated with the binding of co-factors and active sites, and (3) phylogenetic analyses along with sequences from archaeal and bacterial genomes **(Suppl. Fig. S5)**. **b)** Phylum-level relative abundance of microorganisms harbouring denitrification genes across the different soil ecosystems, computed as a proportion of reads mapping to each MAG.

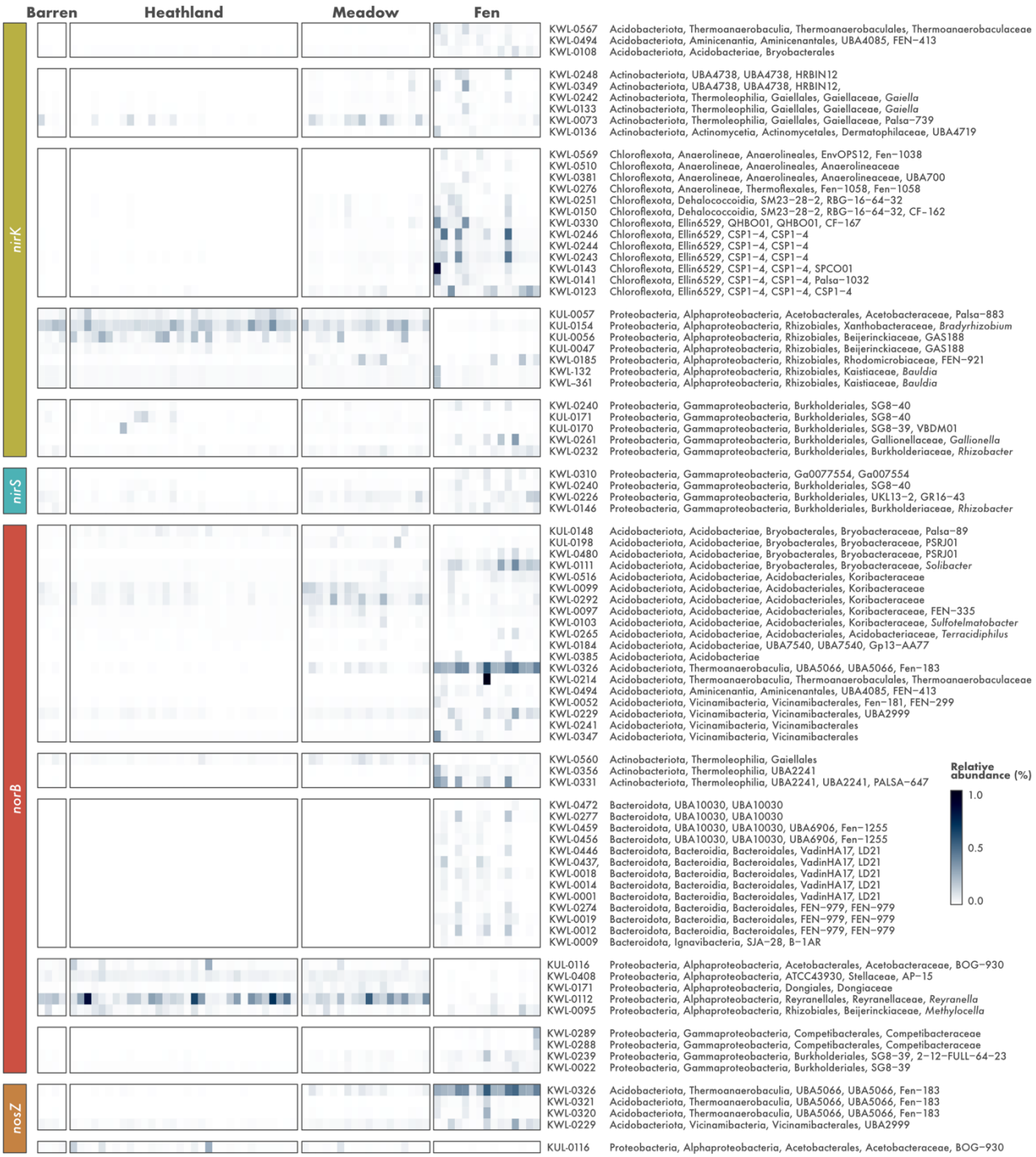

Fig. 4 | Relative abundance of metagenome-assembled genomes (MAGs) harbouring denitrification genes across different soil ecosystems in the tundra. MAGs were recovered from soils in Kilpisjärvi, northern Finland, and annotated for genes encoding the nitrite (*nirK*/*nirS*), nitric oxide (*norB*), and nitrous oxide (*nosZ*) reductases using a three-step approach. Relative abundances were computed as a proportion of reads mapping to each MAG. MAG taxonomy is based on the Genome Taxonomy Database (GTDB) release 05-RS95.

399 **Microorganisms affiliated with the Chloroflexota lineage Ellin6529 are the**
400 **main denitrifiers *stricto sensu* in fen soils**

401 The reduction of NO_2^- to NO, performed by microorganisms harbouring the *nirK* or *nirS* genes,
402 is the hallmark step of denitrification and is often referred to as denitrification *stricto sensu* as
403 it involves the conversion of a soluble substrate to a gaseous product thus leading to the removal
404 of N from the system [12]. Of the 110 Kilpisjärvi MAGs harbouring genes involved in
405 denitrification, 46 contained *nirK*/*nirS* genes and are thus potential denitrifiers *stricto sensu*
406 **(Fig. 3a)**. These belonged mainly to the bacterial phyla Chloroflexota, Actinobacteriota, and
407 Proteobacteria (classes Alpha- and Gammaproteobacteria). Most MAGs (n = 43) contained the
408 *nirK* gene, which encodes the copper-containing form of Nir **(Suppl. Fig. S5a)**. The *nirS* gene
409 encoding the cytochrome cd_1-containing form of Nir was present in four Gammaproteobacteria
410 MAGs **(Suppl. Fig. S5b)**, including one MAG that contained both genes.

411 The composition of potential denitrifier *stricto sensu* communities differed across the ecosystems
412 **(Fig. 3b)**. MAGs belonging to the Alphaproteobacteria class of the Proteobacteria were the most
413 abundant in the barren, heathland, and meadow soils, particularly the MAG KUL-0154
414 assigned to the genera *Bradyrhizobium* **(Fig. 4)**. Two other Alphaproteobacteria MAGs that do
415 not correspond to formally described genera in the families Acetobacteraceae and
416 Beijerinckiaceae (KUL-0057 and KUL-0056, respectively) were also found at high abundances.
417 In addition, one Actinobacteriota MAG assigned to an uncharacterized genus in the family
418 Gaiellaceae (KWL-0073), was abundant in the meadow soils. On the other hand, fen
419 communities were dominated by MAGs belonging to the phylum Chloroflexota **(Fig. 3b)**, which
420 included seven MAGs assigned to the class-level lineage Ellin6529 **(Fig. 4)**.

421 None of the Ellin6529 MAGs that were dominant in the fen communities contained the key
422 genes involved in autotrophic carbon fixation, dissimilatory sulfate reduction, dissimilatory
423 nitrate reduction to ammonia, and nitrogen fixation **(Suppl. Table S3)**. Analysis of genes
424 encoding terminal oxidases involved in the aerobic respiratory electron chain revealed that all
425 seven Ellin6529 MAGs harboured the *coxABC* genes encoding the *aa3*-type cytochrome c
426 oxidase**.** Four MAGs also contained the *cydAB* genes encoding the cytochrome *bd* ubiquinol
427 oxidase, a terminal oxidase with high affinity for oxygen that also plays a role in preventing the
428 inactivation of oxygen-sensitive enzymes and protecting against oxidative and nitrosative
429 stress, toxic compounds such as cyanide, and other stress conditions such as high temperature
430 and high pH [79, 80]. The dominant MAGs in the barren, heathland, and meadow soils encoded
431 a different set of aerobic terminal oxidases. In addition to the *cydAB* genes, the MAGs KUL-
432 0057 and KUL-0154 also contained the *cyoABCD* genes encoding the cytochrome o ubiquinol

433 oxidase, which is the main terminal oxidase under highly aerobic conditions [81], and KUL-0057
434 also contained genes encoding the *cbb3*-type cytochrome c oxidase, a terminal oxidase with high
435 affinity for oxygen [82]. Genes involved in the Calvin cycle (e.g., *rbcL*, *rbcS*, and *prkB*) were
436 found in the *Bradyrhizobium* MAG (KUL-0154), and none of the key genes for autotrophic
437 carbon fixation pathways were present in the other Alphaproteobacteria MAGs that were
438 dominant in the barren, heathland, and meadow soils.

439 Acidobacteriota with the potential to reduce NO and N_2O are abundant in the fens

440 The stepwise reduction of NO to N_2O and N_2 carried out by microorganisms containing the *norB*
441 and *nosZ* genes, respectively, represents the final step of denitrification and the main biotic
442 control on N_2O emissions. Soil denitrification rates depend on multiple environmental
443 conditions such as adequate moisture and inorganic N availability, but whether it results in the
444 emission of N_2O or N_2 is ultimately linked to a balance between the activity of NO and N_2O
445 reducers [11, 15]. *norB* and *nosZ* genes were identified in 62 and 9 Kilpisjärvi MAGs,
446 respectively, belonging mostly to the phyla Actinobacteriota, Bacteroidota, Acidobacteriota, and
447 Proteobacteria (class Alphaproteobacteria) **(Fig. 3a)**. Apart from one Gemmatimonadota and
448 one Acidobacteriota MAG, *norB*- and *nosZ*-containing MAGs were almost exclusively non-
449 denitrifiers *stricto sensu*, i.e., they did not harbour the *nirK*/*nirS* genes involved in the reduction
450 of NO_2^- to NO. Most MAGs (n = 48) harboured a *norB* gene encoding the monomeric, quinol-
451 dependent form of Nor (qNor), while the remaining MAGs (n = 8) encoded the cytochrome
452 c-dependent Nor (cNor) **(Suppl. Fig. S5c)**. In regards to the *nosZ* gene, most MAGs (n = 6)
453 contained sequences affiliated with the clade II (also known as atypical) NosZ [14, 15, 27]
454 **(Suppl. Fig. S5d)**. Only four MAGs contained both the *norB* and *nosZ* genes and thus have the
455 potential to reduce NO completely to N_2 **(Fig. 3a)**.

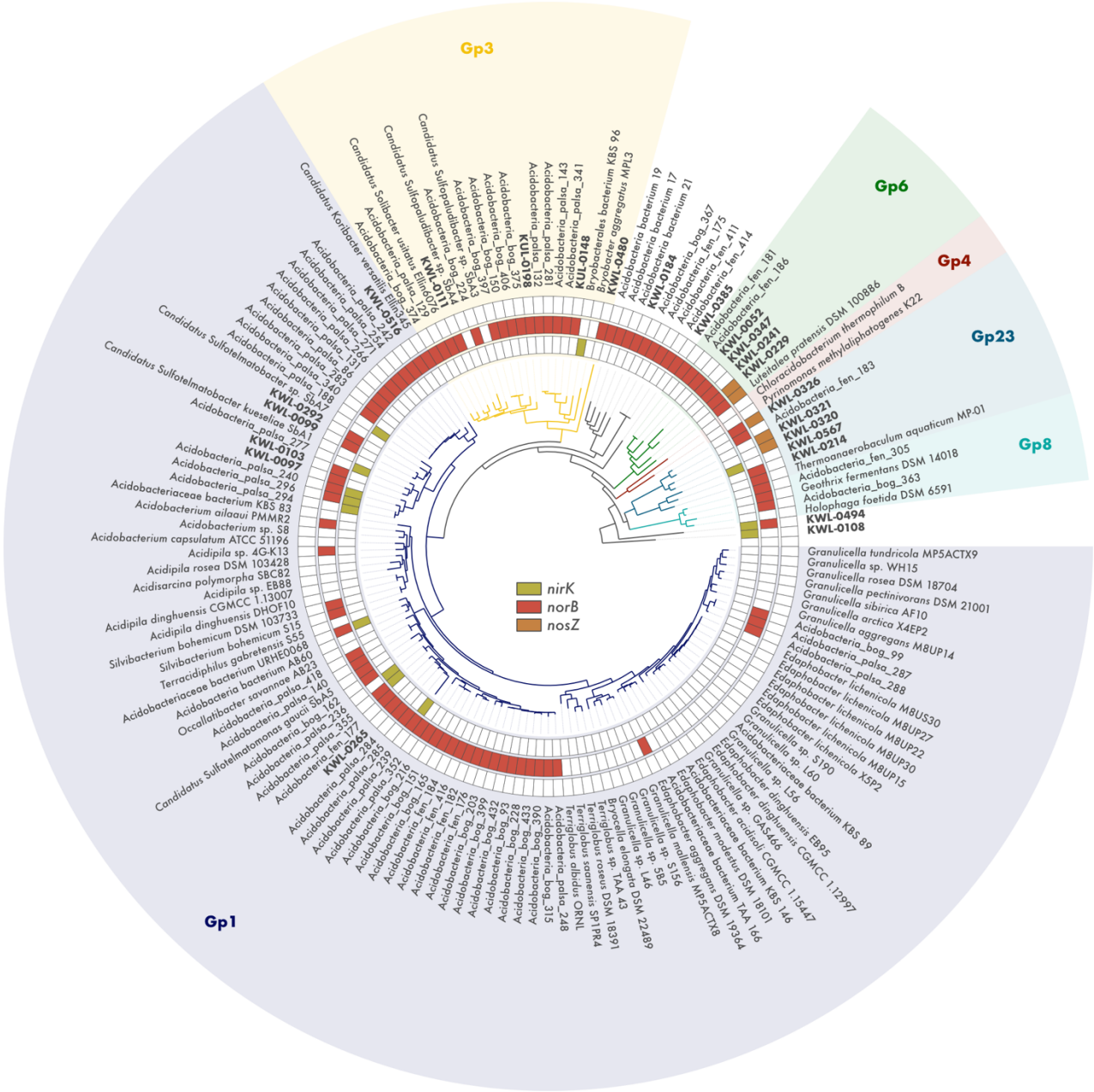

Fig. 5 | Metabolic potential for denitrification among members of the phylum Acidobacteriota. Phylogenomic analysis of 85 Acidobacteriota metagenome-assembled genomes (MAGs) containing denitrification genes recovered from tundra soils in Kilpisjärvi (northern Finland) and Stordalen Mire (northern Sweden), and 69 genomes of Acidobacteriota strains and candidate taxa. Maximum likelihood tree based on concatenated alignments of 23 ribosomal proteins and rooted with *Escherichia coli* ATCC 11775 (not shown). Genes encoding the nitrite (*nirK*), nitric oxide (*norB*), and nitrous oxide (*nosZ*) reductases were annotated using a three-step approach to avoid false positives (see methods).

464 As observed for the denitrifier *stricto sensu* communities, the communities of potential NO and
465 N_2O reducers also differed between the ecosystems **(Fig. 3b)**. MAGs assigned to the
466 Alphaproteobacteria class of the Proteobacteria were the most abundant in the barren,
467 heathland, and meadow soils. In particular, the MAG KWL-0112 assigned to the genera
468 *Reyranella* was the dominant *norB*-containing MAG, while KUL-0116 (belonging to an
469 uncharacterized genus in the family Acetobacteraceae) was the dominant MAG harbouring the
470 *nosZ* gene **(Fig. 4)**. On the other hand, fen communities were dominated by Acidobacteriota
471 MAGs **(Fig. 3b)**, particularly the *norB*- and *nosZ*-containing MAG KWL-0326 affiliated with
472 the class Thermoanaerobaculia **(Fig. 4)**. This MAG contained the same set of genes encoding
473 aerobic terminal oxidases as found in the *nirK*-containing Ellin6529 MAGs that were dominant
474 in the fen sites, namely *coxABC* and *cydAB* **(Suppl. Table S3)**. No genes involved in carbon
475 fixation, dissimilatory sulfate reduction, dissimilatory nitrate reduction to ammonia, and
476 nitrogen fixation were found in any of the dominant *norB*- and *nosZ*-containing MAGs.

477 To elucidate the phylogenetic placement of the Acidobacteriota MAGs and to verify if the
478 potential for NO and N_2O reduction is present in other members of this phylum, we analysed
479 all available genomes of Acidobacteriota strains and candidate taxa available on GenBank. This
480 revealed that genes encoding the Nir and Nos enzymes are widespread across the phylum
481 Acidobacteriota **(Fig. 5)**. Genes encoding the Nor enzyme were present in all but one of the six
482 Acidobacteriota subdivisions with genomes from cultured representatives. This included the
483 strains *Acidobacterium ailaaui* PMMR2 (subdivision Gp1), *Acidipila* sp. 4G-K13 (Gp1),
484 *Silvibacterium bohemicum* DSM 103733 and *S. bohemicum* S15 (Gp1), Acidobacteriaceae
485 bacterium URHE0068 (Gp1), *Edaphobacter aggregans* DSM 19364 (Gp1), *Luteitalea pratensis*
486 DSM 100886 (Gp6), *Geothrix fermentans* DSM 14018 (Gp8), and *Thermoanaerobaculum*
487 *aquaticum* MP-01 (Gp23), as well as the candidate taxa *Candidatus* Koribacter versatilis
488 Ellin345 (Gp1), *Candidatus* Sulfotelmatomonas gaucii SbA5 (Gp1), and *Candidatus* Solibacter
489 usitatus Ellin6076 (Gp3). On the other hand, genes encoding the Nos enzyme were found only
490 in members of the subdivisions Gp6 and Gp23.

491 Discussion

492 The 796 MAGs obtained in the present study by a manual binning and curation effort represent
493 one of the largest genomic catalogues of microorganisms from tundra soils to date. Earlier gene-
494 centric investigations have revealed the potential for complete denitrification in tundra soils
495 [22, 83], however, these approaches fail to reveal the wider genomic context of the genes involved
496 in this pathway. By applying the genome-resolved metagenomics approach, we traced

497 denitrification genes to specific microbial populations, thereby allowing a detailed investigation
498 of the genomic makeup of potential denitrifiers in tundra soils. This approach also enabled us
499 to access the genomes of uncultured, poorly characterized taxa, which comprise the majority of
500 the microorganisms in soils and other complex ecosystems [33, 34].

501 Our genome-resolved survey revealed that denitrification across different tundra soil
502 ecosystems is dominated by microorganisms with truncated denitrification pathways (i.e.,
503 harbouring only a subset of the genes required for complete denitrification), most of which
504 represent poorly characterized taxa without cultured representatives. The congruence of these
505 findings in both our original dataset of northern Finland soils and a re-analysis of a
506 comprehensive metagenomic dataset from soils in northern Sweden [37] suggests that
507 truncated denitrification pathways are not a methodological artifact arising from the metabolic
508 reconstruction of fragmented genomes. Indeed, recent genome-resolved investigations have
509 shown that cross-feeding between microorganisms with truncated metabolic pathways, also
510 known as metabolic handoffs, are the norm across a wide range of ecosystems such as grassland
511 soil, aquifer sediment, groundwater, and the ocean, and not only in relation to denitrification
512 but other redox transformations as well [30, 84, 85]. Although it has been established that
513 denitrification is a community effort performed by different microbial populations [12–15], these
514 genome-resolved metagenomic studies are beginning to reveal a more in-depth, ecosystem-
515 centric representation of the denitrification pathway. In addition to their predominance in
516 genomic databases [14], it appears that truncated denitrifiers are also dominant within defined
517 ecosystems across various terrestrial and aquatic biomes, including the tundra. It has been
518 suggested that the partitioning of metabolic pathways across different populations via metabolic
519 handoffs is advantageous as it eliminates competition between enzymes accelerating substrate
520 consumption [15, 31] and provides flexibility and resilience to the communities in face of
521 environmental disturbances [30]. We further hypothesize that the predominance of
522 denitrification pathways characterized mostly by metabolic handoffs in tundra soils could be
523 related to N limitation. If metabolic handoffs enable a more effective substrate consumption as
524 previously suggested [15, 31], truncated denitrification pathways would be favoured in tundra
525 soils which are mostly N limited but undergo rapid surges in N availability, e.g., during the
526 spring melting season [86].

527 Tundra ecosystems are typically heterogeneous. Previous studies in the Kilpisjärvi region have
528 shown that soil properties such as pH and moisture do not have any strong relationship with
529 the macrotopography of the area (50–500 m scale). Instead, environmental variation is
530 controlled by the fine-scale mesotopographic variation of the relief (2–20 m scale), resulting in
531 a mosaic of different soil ecosystems with contrasting vegetation [40, 75–78]. Our results showed

532 that denitrifier communities in the tundra differ between drier upland ecosystems (barren,
533 heathland, and meadow soils) and water-logged fens. This is likely related to differences in soil
534 moisture affecting oxygen availability in these ecosystems. The dominant denitrifier
535 populations in the oxic dry upland soils, related to the genera *Bradyrhizobium*, *Reyranella*, and
536 other uncharacterized genera in the class Alphaproteobacteria, encoded aerobic terminal
537 oxidases that are active under highly aerobic conditions as well as oxidases with high oxygen
538 affinity [81, 82]. The former likely provides an adaptive advantage in these soils by allowing
539 rapid aerobic growth under standard conditions of high oxygen availability, and the latter would
540 sustain growth in microoxic niches within the soil matrix and during periods of reduced oxygen
541 availability (e.g., during the spring melting season).

542 On the other hand, fen soils are continuously inundated because they are located at lower
543 topographic positions where the water table is permanently at or near the soil surface. The
544 result is a mostly anoxic environment due to the slow rate at which oxygen diffuses into the
545 water-logged soil, favouring reduced rather than oxidized soil chemistry. In line with this, we
546 found a predominance of anaerobic processes in the fens, including a higher abundance of genes
547 involved in denitrification, sulfate reduction, and methanogenesis, the latter supported by *in*
548 *situ* measurements showing net CH_4 emission at the fen sites. Communities of potential
549 denitrifiers in the fen soils were dominated by somewhat enigmatic taxa, namely potential NO_2^-
550 reducers affiliated with the class Ellin6529 of the Chloroflexota and NO/N_2O reducers assigned
551 to the subdivision Gp23 of the Acidobacteriota. Both groups are major members of microbial
552 communities in soils worldwide [87], and RNA-based investigations have shown that they are
553 active in tundra soils during both summer and winter seasons [40, 88]. *Thermoanaerobaculum*
554 *aquaticum* MP-01, the only cultivated member of the Acidobacteriota subdivision Gp23, is a
555 strictly anaerobic bacterium that has been shown to use Fe and Mn, but not NO_3^- nor NO_2^-, as
556 electron acceptors in anaerobic respiration [89]. However, studies investigating the use of
557 nitrogen oxides in anaerobic respiration usually provide soluble NO_3^- or NO_2^- as electron
558 acceptors, not the gases NO and N_2O, which bias against truncated denitrifiers that do not
559 contain the *narG* and *nirK*/*nirS* genes [90]. Ellin6529 – formerly G04 – were first detected by
560 culture-independent methods in alpine tundra wet meadow soil in the Colorado Rocky
561 Mountains, USA [91], and later isolated in a study targeting slow-growing and mini-colony
562 forming bacteria from Australian agricultural soil [92]. However, their ecological, physiological,
563 and metabolic preferences remain largely unknown. Their genomic composition and high
564 abundance in the water-logged, anoxic fen soils suggest that the Ellin6529 and Gp23
565 populations found in this study are likely able to grow anaerobically with the use of NO and
566 N_2O as electron acceptors. However, it is known that in addition to their role in anaerobic

respiration, NO and N_2O reduction can be used as a detoxification mechanism or as electron sink for metabolism. For example, the aerobe *Gemmatimonas aurantica* T-27 is not able to grow on N_2O alone, but can use N_2O as electron acceptor transiently when oxygen is depleted [93].

In addition to microbial community structure, differences in N_2O fluxes observed between upland and fen soils also appear to be linked to soil moisture. Some of the drier upland sites investigated were hotspots of N_2O consumption. This is particularly interesting for the acidic heathland soils, as low pH is known to impair the expression of the NosZ enzyme thus promoting N_2O emission [94, 95]. On the other hand, fens had close to net-zero N_2O fluxes, which is in line with previous observations for water-saturated soils both in the tundra [7] and worldwide [11, 13]. This has been linked to lower rates of N mineralization and nitrification in anoxic ecosystems, which limit the availability of NO_3^- and NO_2^- and promote complete denitrification, resulting in N_2 as end product rather than N_2O. Indeed, supplementing fen soils in the tundra with NO_3^- and NO_2^- has shown to promote N_2O emissions [96]. Moreover, climate change models predict lowering of the water table in high-latitude wetlands, which could lead to increased N_2O emissions from these ecosystems which contain substantial amounts of both C and N bound to the soil organic matter [97, 98].

Conclusions

A better understanding of denitrification is paramount for our ability to model N_2O emissions and mitigate climate change. High-latitude environments in particular have experienced amplified warming in recent decades, a trend that is likely to continue in the coming centuries. As mechanisms of GHG emissions are very climate sensitive, the contribution of tundra soils to global GHG atmospheric levels is thus predicted to increase in the future leading to a positive feedback loop. Compared with CO_2 and CH_4, measurements of N_2O fluxes in tundra soils are sparse and are rarely coupled with a characterization of the microorganisms involved, making the magnitude and drivers of N_2O fluxes across the polar regions uncertain. While microorganisms with truncated denitrification pathways appear to dominate the denitrifier communities investigated here, the potential for complete denitrification was present at the ecosystem level. In addition to a better monitoring of N_2O emissions throughout the tundra biome, our results suggest that a better understanding of the contribution of tundra soil to global N_2O levels relies on the elucidation of the regulatory mechanisms of metabolic handoffs in communities dominated by truncated denitrifiers.

Declarations

Ethics approval and consent to participate

Not applicable.

Consent for publication

Not applicable.

Availability of data and materials

Raw metagenomic data and assembled MAGs have been submitted to the European Nucleotide Archive (ENA) under the project PRJEB41762. All the code used can be found in https://github.com/ArcticMicrobialEcology/Kilpisjarvi-MAGs.

Competing interests

The authors declare that they have no competing interests.

Funding

This work was funded by the Academy of Finland (grants 314114 and 335354) and the University of Helsinki. SV was funded by the Microbiology and Biotechnology Doctoral Programme (MBDP). AMV was funded by the Academy of Finland (grant 286950), the Otto Malm Foundation, and the Gordon and Betty Moore Foundation (grant 8414). MEM was supported by the Academy of Finland (grants 314630 and 317054).

Author contributions

JH and ML designed the research; SV and JH performed nucleic acid extraction and metagenomic library preparation; AMV and MEM designed and performed the GHG flux measurements and analyses; ISP analysed the data and wrote the manuscript; EER and TOD contributed with the analyses; all authors contributed to the final version of the manuscript.

Acknowledgements

We would like to acknowledge CSC – IT Centre for Science for providing the necessary computing resources and Kimmo Mattila for IT support; the staff from the Kilpisjärvi Biological Station, Tanja Orpana, Aino Rutanen, Anniina Sarekoski, Johanna Kerttula, and the members of the BioGeoClimate Modelling Lab for assistance with fieldwork and soil characterization; Jillian Banfield and Christina Biasi for helpful discussion; Laura Cappelatti for proof-reading

the manuscript; Murat Eren, Sebastian Lücker, Donovan Parks, and Antonios Kioukis for tips, recommendations, and troubleshooting; and all anonymous reviewers who provided important insights to the original manuscript.

References

1. IPCC, editor. Climate Change 2013: The Physical Science Basis. Contribution of Working Group I to the Fifth Assessment Report of the Intergovernmental Panel on Climate Change. Cambridge: Cambridge University Press; 2013.

2. Tian H, Xu R, Canadell JG, Thompson RL, Winiwarter W, Suntharalingam P, et al. A comprehensive quantification of global nitrous oxide sources and sinks. Nature. 2020;586:248–56.

3. Repo ME, Susiluoto S, Lind SE, Jokinen S, Elsakov V, Biasi C, et al. Large N2O emissions from cryoturbated peat soil in tundra. Nat Geosci. 2009;2:189–92.

4. Marushchak ME, Pitkämäki A, Koponen H, Biasi C, Seppälä M, Martikainen PJ. Hot spots for nitrous oxide emissions found in different types of permafrost peatlands. Glob Change Biol. 2011;17:2601–14.

5. Stewart KJ, Grogan P, Coxson DS, Siciliano SD. Topography as a key factor driving atmospheric nitrogen exchanges in arctic terrestrial ecosystems. Soil Biol Biochem. 2014;70:96–112.

6. Voigt C, Marushchak ME, Lamprecht RE, Jackowicz-Korczyński M, Lindgren A, Mastepanov M, et al. Increased nitrous oxide emissions from Arctic peatlands after permafrost thaw. Proc Natl Acad Sci. 2017;114:6238–43.

7. Voigt C, Marushchak ME, Abbott BW, Biasi C, Elberling B, Siciliano SD, et al. Nitrous oxide emissions from permafrost-affected soils. Nat Rev Earth Environ. 2020;1:420–34.

8. Schuur EAG, McGuire AD, Schädel C, Grosse G, Harden JW, Hayes DJ, et al. Climate change and the permafrost carbon feedback. Nature. 2015;520:171–9.

9. Hugelius G, Loisel J, Chadburn S, Jackson RB, Jones M, MacDonald G, et al. Large stocks of peatland carbon and nitrogen are vulnerable to permafrost thaw. Proc Natl Acad Sci. 2020;117:20438–46.

10. Post E, Alley RB, Christensen TR, Macias-Fauria M, Forbes BC, Gooseff MN, et al. The polar regions in a 2°C warmer world. Sci Adv. 2019;5:eaaw9883.

656 11. Butterbach-Bahl K, Baggs EM, Dannenmann M, Kiese R, Zechmeister-Boltenstern S.
657 Nitrous oxide emissions from soils: how well do we understand the processes and their controls?
658 Philos Trans R Soc B Biol Sci. 2013;368:20130122.

659 12. Zumft WG. Cell biology and molecular basis of denitrification. Microbiol Mol Biol Rev
660 MMBR. 1997;61:533–616.

661 13. Wallenstein MD, Myrold DD, Firestone M, Voytek M. Environmental controls on
662 denitrifying communities and denitrification rates: insights from molecular methods. Ecol Appl.
663 2006;16:2143–52.

664 14. Graf DRH, Jones CM, Hallin S. Intergenomic Comparisons Highlight Modularity of the
665 Denitrification Pathway and Underpin the Importance of Community Structure for N2O
666 Emissions. PLoS ONE. 2014;9:e114118.

667 15. Hallin S, Philippot L, Löffler FE, Sanford RA, Jones CM. Genomics and Ecology of Novel
668 N2O-Reducing Microorganisms. Trends Microbiol. 2018;26:43–55.

669 16. Liu X-Y, Koba K, Koyama LA, Hobbie SE, Weiss MS, Inagaki Y, et al. Nitrate is an important
670 nitrogen source for Arctic tundra plants. Proc Natl Acad Sci. 2018;115:3398–403.

671 17. Kou D, Yang G, Li F, Feng X, Zhang D, Mao C, et al. Progressive nitrogen limitation across
672 the Tibetan alpine permafrost region. Nat Commun. 2020;11:3331.

673 18. Yergeau E, Kang S, He Z, Zhou J, Kowalchuk GA. Functional microarray analysis of
674 nitrogen and carbon cycling genes across an Antarctic latitudinal transect. ISME J. 2007;1:163–
675 79.

676 19. Yergeau E, Hogues H, Whyte LG, Greer CW. The functional potential of high Arctic
677 permafrost revealed by metagenomic sequencing, qPCR and microarray analyses. ISME J.
678 2010;4:1206–14.

679 20. Palmer K, Biasi C, Horn MA. Contrasting denitrifier communities relate to contrasting N2O
680 emission patterns from acidic peat soils in arctic tundra. ISME J. 2012;6:1058–77.

681 21. Dai H-T, Zhu R-B, Sun B-W, Che C-S, Hou L-J. Effects of Sea Animal Activities on Tundra
682 Soil Denitrification and nirS- and nirK-Encoding Denitrifier Community in Maritime
683 Antarctica. Front Microbiol. 2020;11:573302.

684 22. Ortiz M, Bosch J, Coclet C, Johnson J, Lebre P, Salawu-Rotimi A, et al. Microbial Nitrogen
685 Cycling in Antarctic Soils. Microorganisms. 2020;8:1442.

686 23. Brummell ME, Farrell RE, Siciliano SD. Greenhouse gas soil production and surface fluxes
687 at a high arctic polar oasis. Soil Biol Biochem. 2012;52:1–12.

688 24. Chapuis-Lardy L, Wrage N, Metay A, Chotte J-L, Bernoux M. Soils, a sink for N_2O? A
689 review. Glob Change Biol. 2007;13:1–17.

690 25. Bakken LR, Bergaust L, Liu B, Frostegård Å. Regulation of denitrification at the cellular
691 level: a clue to the understanding of N_2O emissions from soils. Philos Trans R Soc B Biol Sci.
692 2012;367:1226–34.

693 26. Philippot L, Andert J, Jones CM, Bru D, Hallin S. Importance of denitrifiers lacking the
694 genes encoding the nitrous oxide reductase for N2O emissions from soil: role of denitrifier
695 diversity for N2O fluxes. Glob Change Biol. 2011;17:1497–504.

696 27. Sanford RA, Wagner DD, Wu Q, Chee-Sanford JC, Thomas SH, Cruz-Garcia C, et al.
697 Unexpected nondenitrifier nitrous oxide reductase gene diversity and abundance in soils. Proc
698 Natl Acad Sci. 2012;109:19709–14.

699 28. Jones CM, Graf DR, Bru D, Philippot L, Hallin S. The unaccounted yet abundant nitrous
700 oxide-reducing microbial community: a potential nitrous oxide sink. ISME J. 2013;7:417–26.

701 29. Jones CM, Spor A, Brennan FP, Breuil M-C, Bru D, Lemanceau P, et al. Recently identified
702 microbial guild mediates soil N2O sink capacity. Nat Clim Change. 2014;4:801–5.

703 30. Anantharaman K, Brown CT, Hug LA, Sharon I, Castelle CJ, Probst AJ, et al. Thousands
704 of microbial genomes shed light on interconnected biogeochemical processes in an aquifer
705 system. Nat Commun. 2016;7:13219.

706 31. Lilja EE, Johnson DR. Segregating metabolic processes into different microbial cells
707 accelerates the consumption of inhibitory substrates. ISME J. 2016;10:1568–78.

708 32. Yu T, Zhuang Q. Quantifying global N2O emissions from natural ecosystem soils using trait-
709 based biogeochemistry models. Biogeosciences. 2019;16:207–22.

710 33. Rappé MS, Giovannoni SJ. The Uncultured Microbial Majority. Annu Rev Microbiol.
711 2003;57:369–94.

712 34. Steen AD, Crits-Christoph A, Carini P, DeAngelis KM, Fierer N, Lloyd KG, et al. High
713 proportions of bacteria and archaea across most biomes remain uncultured. ISME J.
714 2019;13:3126–30.

715 35. Mackelprang R, Waldrop MP, DeAngelis KM, David MM, Chavarria KL, Blazewicz SJ, et
716 al. Metagenomic analysis of a permafrost microbial community reveals a rapid response to thaw.
717 Nature. 2011;480:368–71.

718 36. Hultman J, Waldrop MP, Mackelprang R, David MM, McFarland J, Blazewicz SJ, et al.
719 Multi-omics of permafrost, active layer and thermokarst bog soil microbiomes. Nature.
720 2015;521:208–12.

721 37. Woodcroft BJ, Singleton CM, Boyd JA, Evans PN, Emerson JB, Zayed AAF, et al. Genome-
722 centric view of carbon processing in thawing permafrost. Nature. 2018;560:49–54.

723 38. Pirinen P, Simola H, Aalto J, Kaukoranta J-P, Karlsson P, Ruuhela R. Climatological
724 statistics of Finland 1981–2010. Helsinki: Finnish Meteorological Institute; 2012.

725 39. Livingston GP, Hutchinson GL. Enclosure-based measurement of trace gas exchange:
726 applications and sources of error. In: Biogenic trace gases: Measuring emissions from soil and
727 water. Oxford, United Kingdom: Blackwell Science. p. 14–51.

728 40. Viitamäki S, Pessi IS, Virkkala A-M, Niittynen P, Kemppinen J, Eronen-Rasimus E, et al.
729 The activity and functions of subarctic soil microbial communities vary across vegetation types.
730 bioRxiv. 2021. https://doi.org/10.1101/2021.06.12.448001.

731 41. Ewels P, Magnusson M, Lundin S, Käller M. MultiQC: summarize analysis results for
732 multiple tools and samples in a single report. Bioinformatics. 2016;32:3047–8.

733 42. Martin M. Cutadapt removes adapter sequences from high-throughput sequencing reads.
734 EMBnet.journal. 2011;17:10.

735 43. Leger A, Leonardi T. pycoQC, interactive quality control for Oxford Nanopore Sequencing.
736 J Open Source Softw. 2019;4:1236.

737 44. Bengtsson-Palme J, Hartmann M, Eriksson KM, Pal C, Thorell K, Larsson DGJ, et al.
738 METAXA 2: improved identification and taxonomic classification of small and large subunit
739 rRNA in metagenomic data. Mol Ecol Resour. 2015;15:1403–14.

740 45. Quast C, Pruesse E, Yilmaz P, Gerken J, Schweer T, Yarza P, et al. The SILVA ribosomal
741 RNA gene database project: improved data processing and web-based tools. Nucleic Acids Res.
742 2012;41:D590–6.

743 46. Schloss PD, Westcott SL, Ryabin T, Hall JR, Hartmann M, Hollister EB, et al. Introducing
744 mothur: Open-Source, Platform-Independent, Community-Supported Software for Describing
745 and Comparing Microbial Communities. Appl Environ Microbiol. 2009;75:7537–41.

746 47. Wang Q, Garrity GM, Tiedje JM, Cole JR. Naïve Bayesian Classifier for Rapid Assignment
747 of rRNA Sequences into the New Bacterial Taxonomy. Appl Environ Microbiol. 2007;73:5261–
748 7.

749 48. Li D, Liu C-M, Luo R, Sadakane K, Lam T-W. MEGAHIT: an ultra-fast single-node solution
750 for large and complex metagenomics assembly via succinct de Bruijn graph. Bioinformatics.
751 2015;31:1674–6.

752 49. Kolmogorov M, Bickhart DM, Behsaz B, Gurevich A, Rayko M, Shin SB, et al. metaFlye:
753 scalable long-read metagenome assembly using repeat graphs. Nat Methods. 2020.
754 https://doi.org/10.1038/s41592-020-00971-x.

755 50. Langmead B, Salzberg SL. Fast gapped-read alignment with Bowtie 2. Nat Methods.
756 2012;9:357–9.

757 51. Li H, Handsaker B, Wysoker A, Fennell T, Ruan J, Homer N, et al. The Sequence
758 Alignment/Map format and SAMtools. Bioinformatics. 2009;25:2078–9.

759 52. Walker BJ, Abeel T, Shea T, Priest M, Abouelliel A, Sakthikumar S, et al. Pilon: An
760 Integrated Tool for Comprehensive Microbial Variant Detection and Genome Assembly
761 Improvement. PLoS ONE. 2014;9:e112963.

762 53. Mikheenko A, Saveliev V, Gurevich A. MetaQUAST: evaluation of metagenome assemblies.
763 Bioinformatics. 2016;32:1088–90.

764 54. Eren AM, Esen ÖC, Quince C, Vineis JH, Morrison HG, Sogin ML, et al. Anvi'o: an advanced
765 analysis and visualization platform for 'omics data. PeerJ. 2015;3:e1319.

766 55. Hyatt D, Chen G-L, LoCascio PF, Land ML, Larimer FW, Hauser LJ. Prodigal: prokaryotic
767 gene recognition and translation initiation site identification. BMC Bioinformatics.
768 2010;11:119.

769 56. Eddy SR. Accelerated Profile HMM Searches. PLoS Comput Biol. 2011;7:e1002195.

770 57. Buchfink B, Xie C, Huson DH. Fast and sensitive protein alignment using DIAMOND. Nat
771 Methods. 2015;12:59–60.

772 58. Parks DH, Chuvochina M, Waite DW, Rinke C, Skarshewski A, Chaumeil P-A, et al. A
773 standardized bacterial taxonomy based on genome phylogeny substantially revises the tree of
774 life. Nat Biotechnol. 2018;36:996–1004.

775 59. Parks DH, Chuvochina M, Chaumeil P-A, Rinke C, Mussig AJ, Hugenholtz P. A complete
776 domain-to-species taxonomy for Bacteria and Archaea. Nat Biotechnol. 2020.
777 https://doi.org/10.1038/s41587-020-0501-8.

778 60. Alneberg J, Bjarnason BS, de Bruijn I, Schirmer M, Quick J, Ijaz UZ, et al. Binning
779 metagenomic contigs by coverage and composition. Nat Methods. 2014;11:1144–6.

780 61. Bowers RM, Kyrpides NC, Stepanauskas R, Harmon-Smith M, Doud D, Reddy TBK, et al.
781 Minimum information about a single amplified genome (MISAG) and a metagenome-assembled
782 genome (MIMAG) of bacteria and archaea. Nat Biotechnol. 2017;35:725–31.

783 62. Aramaki T, Blanc-Mathieu R, Endo H, Ohkubo K, Kanehisa M, Goto S, et al. KofamKOALA:
784 KEGG Ortholog assignment based on profile HMM and adaptive score threshold.
785 Bioinformatics. 2020;36:2251–2.

786 63. Katoh K, Standley DM. MAFFT Multiple Sequence Alignment Software Version 7:
787 Improvements in Performance and Usability. Mol Biol Evol. 2013;30:772–80.

788 64. Okonechnikov K, Golosova O, Fursov M. Unipro UGENE: a unified bioinformatics toolkit.
789 Bioinformatics. 2012;28:1166–7.

790 65. Decleyre H, Heylen K, Tytgat B, Willems A. Highly diverse nirK genes comprise two major
791 clades that harbour ammonium-producing denitrifiers. BMC Genomics. 2016;17:155.

792 66. Li Y, Bali S, Borg S, Katzmann E, Ferguson SJ, Schuler D. Cytochrome cd1 Nitrite
793 Reductase NirS Is Involved in Anaerobic Magnetite Biomineralization in Magnetospirillum
794 gryphiswaldense and Requires NirN for Proper d1 Heme Assembly. J Bacteriol. 2013;195:4297–
795 309.

796 67. Heylen K, Keltjens J. Redundancy and modularity in membrane-associated dissimilatory
797 nitrate reduction in Bacillus. Front Microbiol. 2012;3.

798 68. Price MN, Dehal PS, Arkin AP. FastTree 2 – Approximately Maximum-Likelihood Trees for
799 Large Alignments. PLoS ONE. 2010;5:e9490.

800 69. Woodcroft BJ. CoverM. 2021.

801 70. Li H. Minimap and miniasm: fast mapping and de novo assembly for noisy long sequences.
802 Bioinformatics. 2016;32:2103–10.

803 71. Chaumeil P-A, Mussig AJ, Hugenholtz P, Parks DH. GTDB-Tk: a toolkit to classify genomes
804 with the Genome Taxonomy Database. Bioinformatics. 2019;:btz848.

805 72. Edgar RC. MUSCLE: multiple sequence alignment with high accuracy and high throughput.
806 Nucleic Acids Res. 2004;32:1792–7.

807 73. Zhang H, Yohe T, Huang L, Entwistle S, Wu P, Yang Z, et al. dbCAN2: a meta server for
808 automated carbohydrate-active enzyme annotation. Nucleic Acids Res. 2018;46:W95–101.

809 74. Jain C, Rodriguez-R LM, Phillippy AM, Konstantinidis KT, Aluru S. High throughput ANI
810 analysis of 90K prokaryotic genomes reveals clear species boundaries. Nat Commun.
811 2018;9:5114.

812 75. le Roux PC, Aalto J, Luoto M. Soil moisture's underestimated role in climate change impact
813 modelling in low-energy systems. Glob Change Biol. 2013;19:2965–75.

814 76. Niittynen P, Heikkinen RK, Aalto J, Guisan A, Kemppinen J, Luoto M. Fine-scale tundra
815 vegetation patterns are strongly related to winter thermal conditions. Nat Clim Change. 2020.
816 https://doi.org/10.1038/s41558-020-00916-4.

817 77. le Roux PC, Pellissier L, Wisz MS, Luoto M. Incorporating dominant species as proxies for
818 biotic interactions strengthens plant community models. J Ecol. 2014;102:767–75.

819 78. Kemppinen J, Niittynen P, Aalto J, le Roux PC, Luoto M. Water as a resource, stress and
820 disturbance shaping tundra vegetation. Oikos. 2019;128:811–22.

821 79. Borisov VB, Gennis RB, Hemp J, Verkhovsky MI. The cytochrome bd respiratory oxygen
822 reductases. Biochim Biophys Acta BBA - Bioenerg. 2011;1807:1398–413.

823 80. Giuffrè A, Borisov VB, Arese M, Sarti P, Forte E. Cytochrome bd oxidase and bacterial
824 tolerance to oxidative and nitrosative stress. Biochim Biophys Acta BBA - Bioenerg.
825 2014;1837:1178–87.

826 81. Dinamarca MA, Ruiz-Manzano A, Rojo F. Inactivation of Cytochrome *o* Ubiquinol Oxidase
827 Relieves Catabolic Repression of the *Pseudomonas putida* GPo1 Alkane Degradation Pathway.
828 J Bacteriol. 2002;184:3785–93.

829 82. Bueno E, Mesa S, Bedmar EJ, Richardson DJ, Delgado MJ. Bacterial Adaptation of
830 Respiration from Oxic to Microoxic and Anoxic Conditions: Redox Control. Antioxid Redox
831 Signal. 2012;16:819–52.

832 83. Makhalanyane TP, Van Goethem MW, Cowan DA. Microbial diversity and functional
833 capacity in polar soils. Curr Opin Biotechnol. 2016;38:159–66.

834 84. Diamond S, Andeer PF, Li Z, Crits-Christoph A, Burstein D, Anantharaman K, et al.
835 Mediterranean grassland soil C–N compound turnover is dependent on rainfall and depth, and
836 is mediated by genomically divergent microorganisms. Nat Microbiol. 2019;4:1356–67.

837 85. Sun X, Ward BB. Novel metagenome-assembled genomes involved in the nitrogen cycle from
838 a Pacific oxygen minimum zone. ISME Commun. 2021;1:26.

86. Westergaard-Nielsen A, Balstrøm T, Treier UA, Normand S, Elberling B. Estimating meltwater retention and associated nitrate redistribution during snowmelt in an Arctic tundra landscape. Environ Res Lett. 2020;15:034025.

87. Delgado-Baquerizo M, Oliverio AM, Brewer TE, Benavent-González A, Eldridge DJ, Bardgett RD, et al. A global atlas of the dominant bacteria found in soil. Science. 2018;359:320–5.

88. Männistö MK, Kurhela E, Tiirola M, Häggblom MM. Acidobacteria dominate the active bacterial communities of Arctic tundra with widely divergent winter-time snow accumulation and soil temperatures. FEMS Microbiol Ecol. 2013;84:47–59.

89. Losey NA, Stevenson BS, Busse H-J, Damsté JSS, Rijpstra WIC, Rudd S, et al. Thermoanaerobaculum aquaticum gen. nov., sp. nov., the first cultivated member of Acidobacteria subdivision 23, isolated from a hot spring. Int J Syst Evol Microbiol. 2013;63 Pt_11:4149–57.

90. Lycus P, Lovise Bøthun K, Bergaust L, Peele Shapleigh J, Reier Bakken L, Frostegård Å. Phenotypic and genotypic richness of denitrifiers revealed by a novel isolation strategy. ISME J. 2017;11:2219–32.

91. Costello EK, Schmidt SK. Microbial diversity in alpine tundra wet meadow soil: novel Chloroflexi from a cold, water-saturated environment. Environ Microbiol. 2006;8:1471–86.

92. Davis KER, Sangwan P, Janssen PH. Acidobacteria, Rubrobacteridae and Chloroflexi are abundant among very slow-growing and mini-colony-forming soil bacteria. Environ Microbiol. 2011;13:798–805.

93. Park D, Kim H, Yoon S. Nitrous Oxide Reduction by an Obligate Aerobic Bacterium, Gemmatimonas aurantiaca Strain T-27. Appl Environ Microbiol. 2017;83.

94. Liu B, Frostegård Å, Bakken LR. Impaired Reduction of N_2O to N_2 in Acid Soils Is Due to a Posttranscriptional Interference with the Expression of *nosZ*. mBio. 2014;5.

95. Samad MS, Biswas A, Bakken LR, Clough TJ, de Klein CAM, Richards KG, et al. Phylogenetic and functional potential links pH and N2O emissions in pasture soils. Sci Rep. 2016;6:35990.

96. Palmer K, Horn MA. Denitrification Activity of a Remarkably Diverse Fen Denitrifier Community in Finnish Lapland Is N-Oxide Limited. PLOS ONE. 2015;10:e0123123.

97. Smith K. The potential for feedback effects induced by global warming on emissions of nitrous oxide by soils. Glob Change Biol. 1997;3:327–38.

98. Kåresdotter E, Destouni G, Ghajarnia N, Hugelius G, Kalantari Z. Mapping the Vulnerability of Arctic Wetlands to Global Warming. Earths Future. 2021;9.

Supplementary Figures

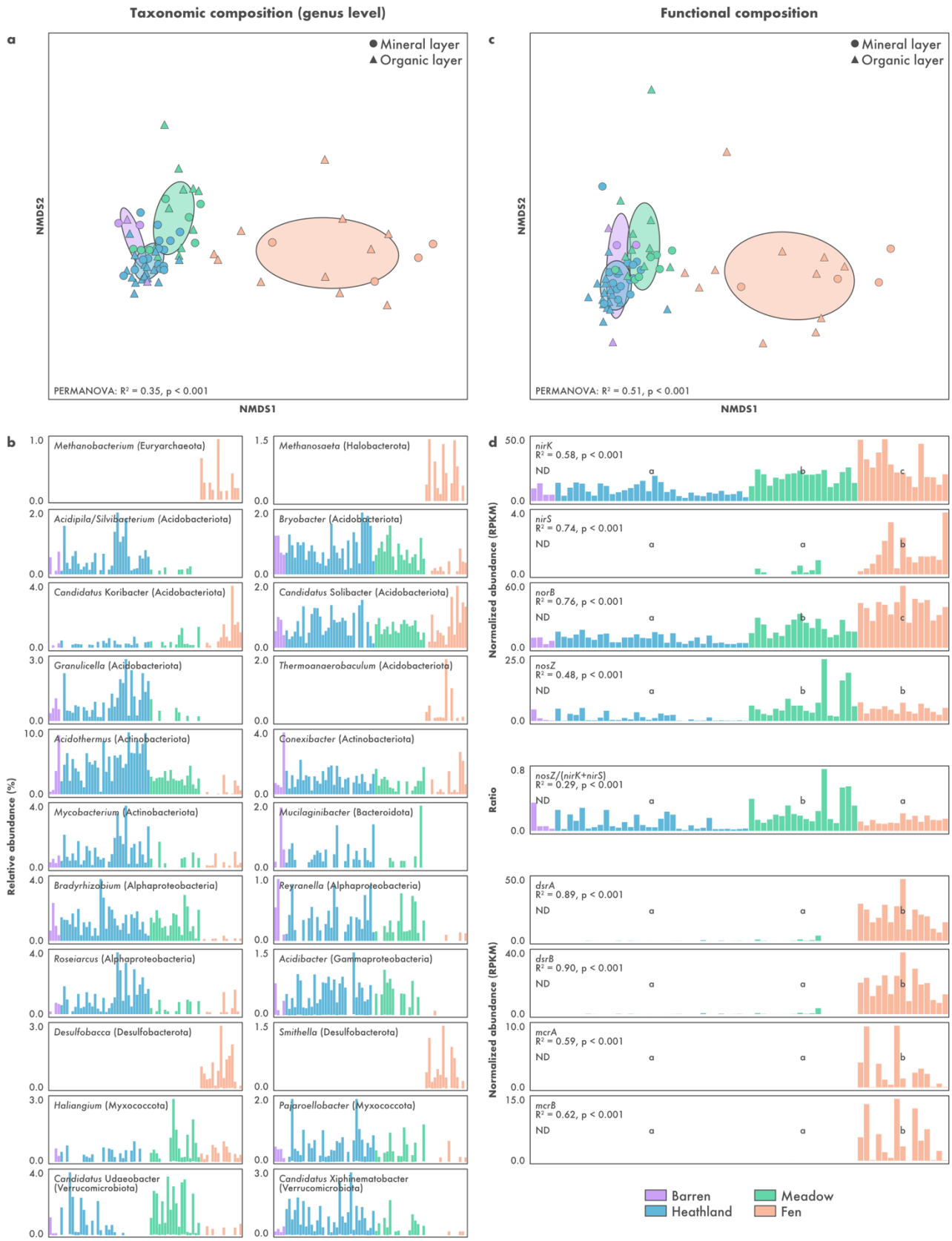

874 **(Previous page) Suppl. Fig. S1 | The microbial diversity of Kilpisjärvi soils as seen**
875 **using a gene-centric approach.** Taxonomic composition was computed based on the
876 annotation of unassembled SSU rRNA gene sequences against the SILVA database. Functional
877 annotation was done by searching assembled genes against the KOfam database. The
878 annotation of putative denitrification genes was confirmed using a phylogenetic approach. **a, c)**
879 Non-metric multidimensional scaling (NMDS) of taxonomic and functional community
880 structure, respectively. Differences between the ecosystems were assessed using permutational
881 ANOVA (PERMANOVA). **b)** Abundance profile of the five most abundant genera in each
882 ecosystem. **d)** Abundance profile of marker genes for denitrification, sulfate reduction, and
883 methanogenesis. Ecosystems followed by different letters are significantly different (one-way
884 ANOVA, $p < 0.05$). Samples from barren soils were not included in the ANOVA procedure due
885 to the limited number of samples (ND: not determined).

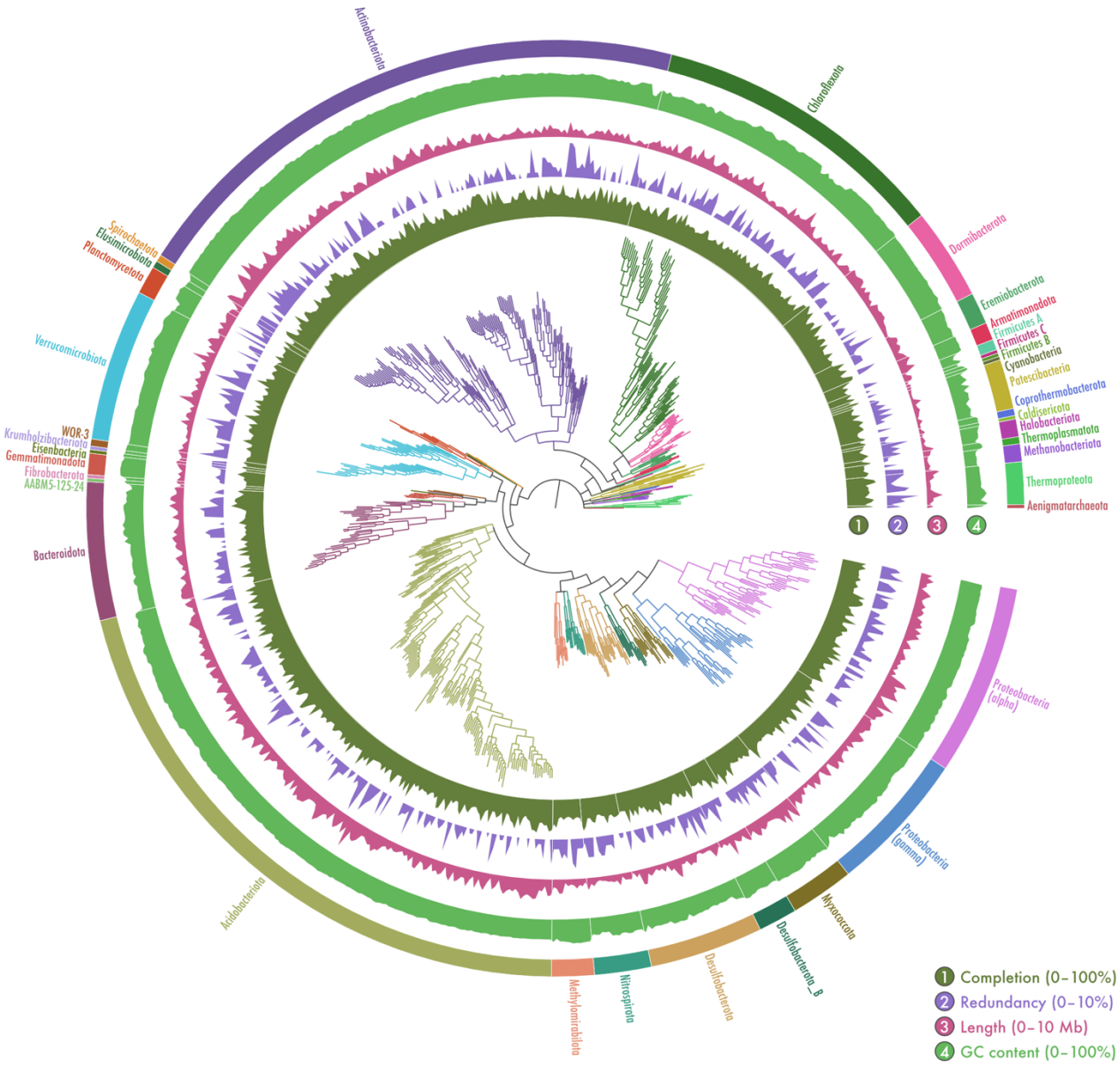

Suppl. Fig. S2 | Genome-resolved metagenomics of tundra soils. Phylogenomic placement and assembly statistics of 796 metagenome-assembled genomes (MAGs) recovered from soils in Kilpisjärvi, northern Finland. Unrooted maximum likelihood tree based on concatenated alignments of amino acid sequences from 122 archaeal and 120 bacterial single-copy genes. Additional information about the MAGs can be found in **Suppl. Table S2**.

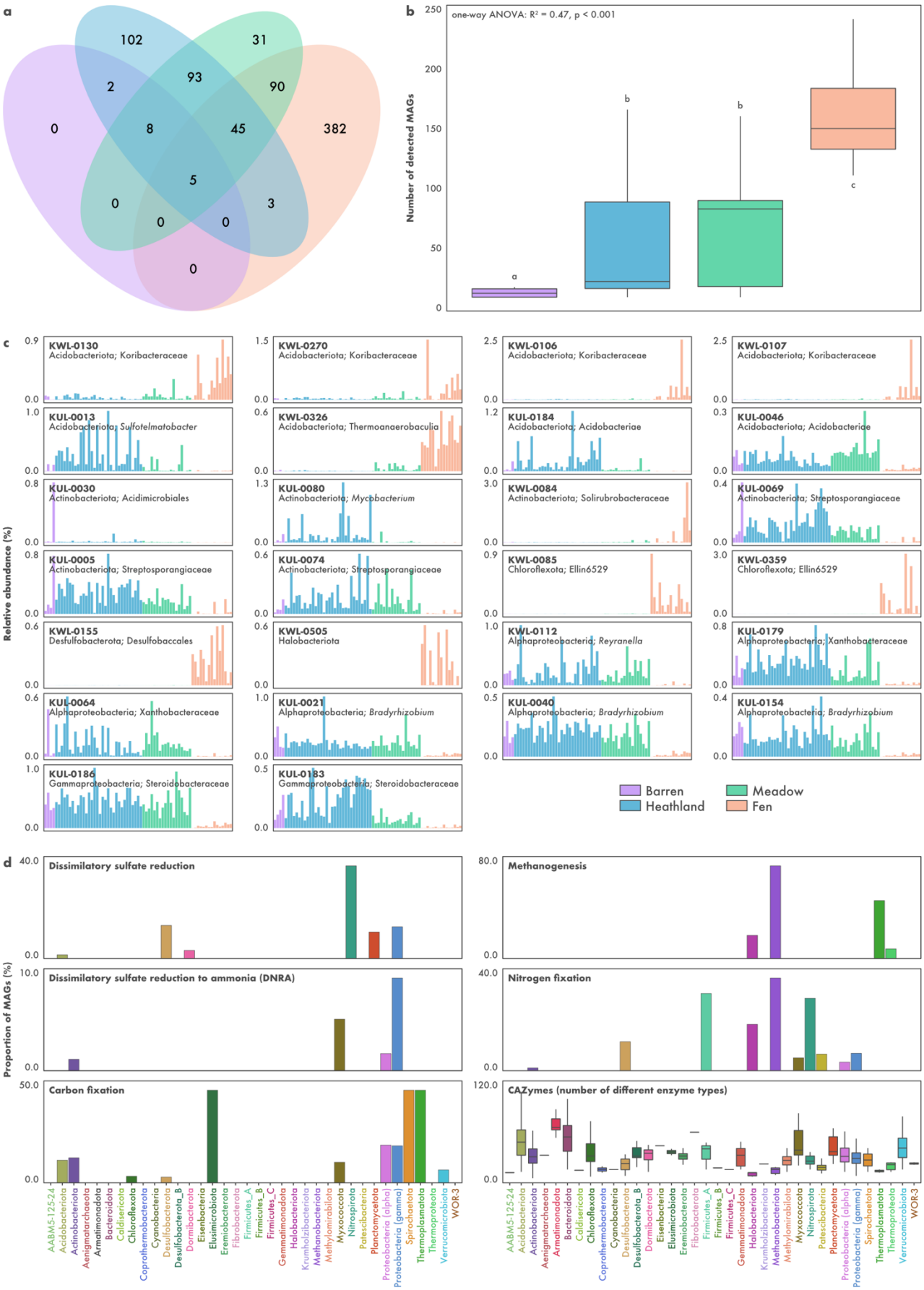
a
102
31
2
93
90
0
8
45
382
5
0
3
0
0
0
b
one-way ANOVA: R² = 0.47, p < 0.001
Number of detected MAGs
250
200
150
100
50
0
a
b
b
c
c
Relative abundance (%)
KWL-0130
Acidobacteriota; Koribacteraceae
KWL-0270
Acidobacteriota; Koribacteraceae
KWL-0106
Acidobacteriota; Koribacteraceae
KWL-0107
Acidobacteriota; Koribacteraceae
KUL-0013
Acidobacteriota; Sulfotelmatobacter
KWL-0326
Acidobacteriota; Thermoanaerobaculia
KUL-0184
Acidobacteriota; Acidobacteriae
KUL-0046
Acidobacteriota; Acidobacteriae
KUL-0030
Actinobacteriota; Acidimicrobiales
KUL-0080
Actinobacteriota; Mycobacterium
KWL-0084
Actinobacteriota; Solirubrobacteraceae
KUL-0069
Actinobacteriota; Streptosporangiaceae
KUL-0005
Actinobacteriota; Streptosporangiaceae
KUL-0074
Actinobacteriota; Streptosporangiaceae
KWL-0085
Chloroflexota; Ellin6529
KWL-0359
Chloroflexota; Ellin6529
KWL-0155
Desfulfobacterota; Desulfobaccales
KWL-0505
Halobacteriota
KWL-0112
Alphaproteobacteria; Reyranella
KUL-0179
Alphaproteobacteria; Xanthobacteraceae
KUL-0064
Alphaproteobacteria; Xanthobacteraceae
KUL-0021
Alphaproteobacteria; Bradyrhizobium
KUL-0040
Alphaproteobacteria; Bradyrhizobium
KUL-0154
Alphaproteobacteria; Bradyrhizobium
KUL-0186
Gammaproteobacteria; Steroidobacteraceae
KUL-0183
Gammaproteobacteria; Steroidobacteraceae
Barren
Heathland
Meadow
Fen
d
Proportion of MAGs (%)
Dissimilatory sulfate reduction
Methanogenesis
Dissimilatory sulfate reduction to ammonia (DNRA)
Nitrogen fixation
Carbon fixation
CAZymes (number of different enzyme types)
AABM5-125-24
Acidobacteriota
Actinobacteriota
Aenigmatarchaeota
Armatimonadota
Bacteroidota
Caldisericota
Chloroflexota
Coprothermobacteriota
Cyanobacteria
Desulfobacterota
Desulfobacterota_B
Dormibacteriota
Eisenbacteria
Elusimicrobiota
Eremiobacteriota
Fibrobacteriota
Firmicutes_A
Firmicutes_B
Firmicutes_C
Gemmatimonadota
Halobacteriota
Krumholzibacteriota
Methanobacteriota
Methylomirabilota
Myxococcota
Nitrospirota
Patescibacteria
Planctomycetota
Proteobacteria (alpha)
Proteobacteria (gamma)
Spirochaetota
Thermoplasmatota
Thermoproteota
Verrucomicrobiota
WOR-3

(Previous page) Suppl. Fig. S3 | Overview of the microbial diversity in Kilpisjärvi soils based on a genome-resolved approach. a) Number of metagenome-assembled genomes (MAGs) shared between the different ecosystems. **b)** Number of detected MAGs across the ecosystems. **c)** Relative abundance of the ten most abundant MAGs in each ecosystem, computed as a proportion of reads mapping to each MAG. **d)** Metabolic potential of the MAGs based on the annotation of genes against the KOfam database. Bar plots represent the proportion of MAGs in each phylum with complete pathways, i.e., containing ≥ 75% of the genes in the pathway. Boxplots of carbohydrate-active enzymes (CAZymes) show the number of different enzyme types identified in each MAG.

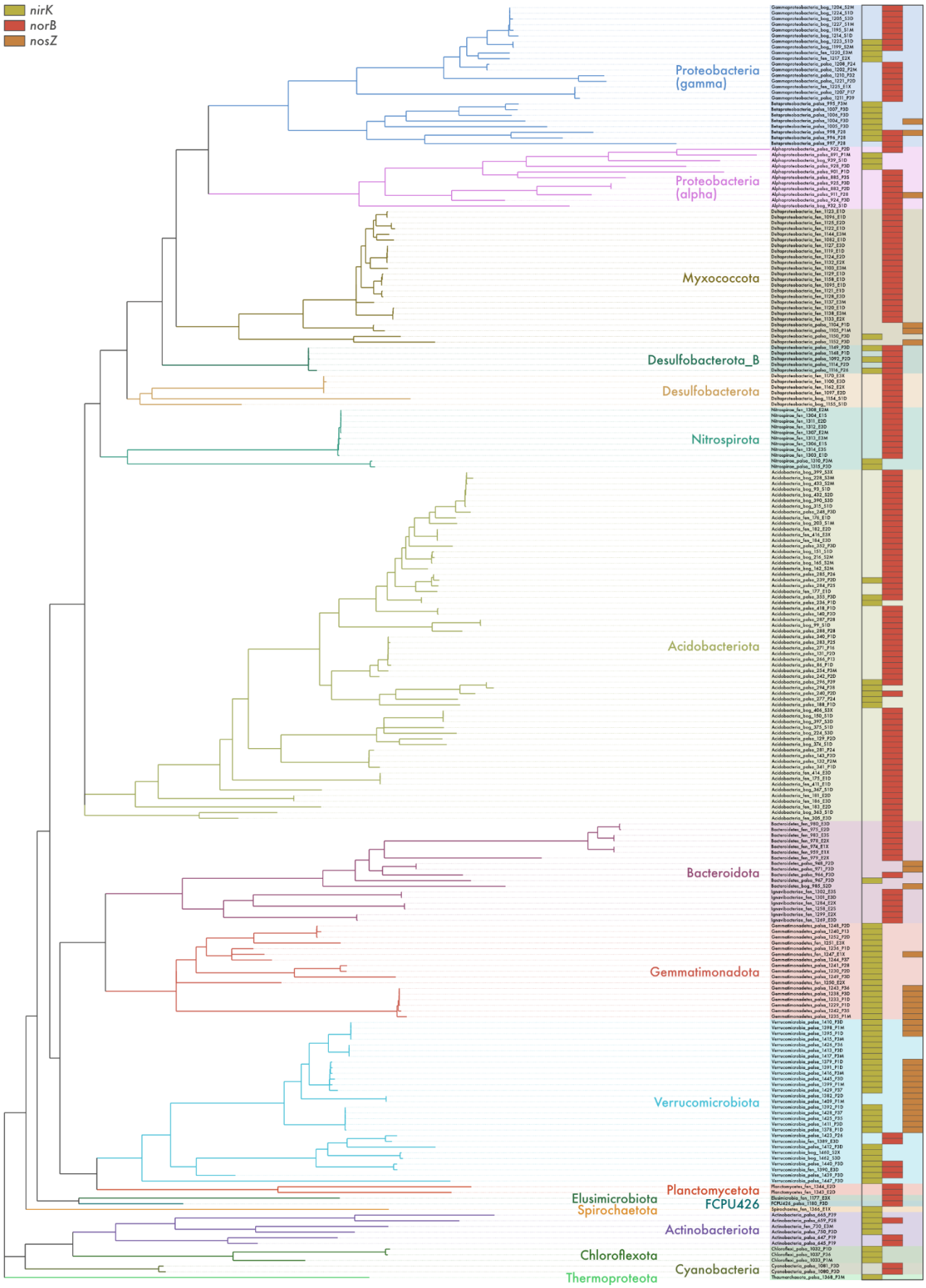
nirK
norB
nosZ
Proteobacteria (gamma)
Proteobacteria (alpha)
Myxococcota
Desulfobacterota_B
Desulfobacterota
Nitrospirota
Acidobacteriota
Bacteroidota
Gemmatimonadota
Verrucomicrobiota
Planctomycetota
Elusimicrobiota
FCPU426
Spirochaetota
Actinobacteriota
Chloroflexota
Cyanobacteria
Thermoproteota

(Previous page) Suppl. Fig. S4 | Metabolic potential for denitrification in Stordalen Mire soils. Distribution of denitrification genes across 225 metagenome-assembled genomes (MAGs) from permafrost peatland, bog, and fen soils in Stordalen Mire, northern Sweden. Genes encoding the nitrite (*nirK*), nitric oxide (*norB*), and nitrous oxide (*nosZ*) reductases were annotated using a three-step approach including (1) identification using hidden Markov models from the KOfam database, (2) manual inspection for the presence of conserved residues at positions associated with the binding of co-factors and active sites, and (3) phylogenetic analyses along with sequences from archaeal and bacterial genomes. Phylogenomic analysis of MAGs was done based on concatenated alignments of amino acid sequences from 122 archaeal and 120 bacterial single-copy genes.

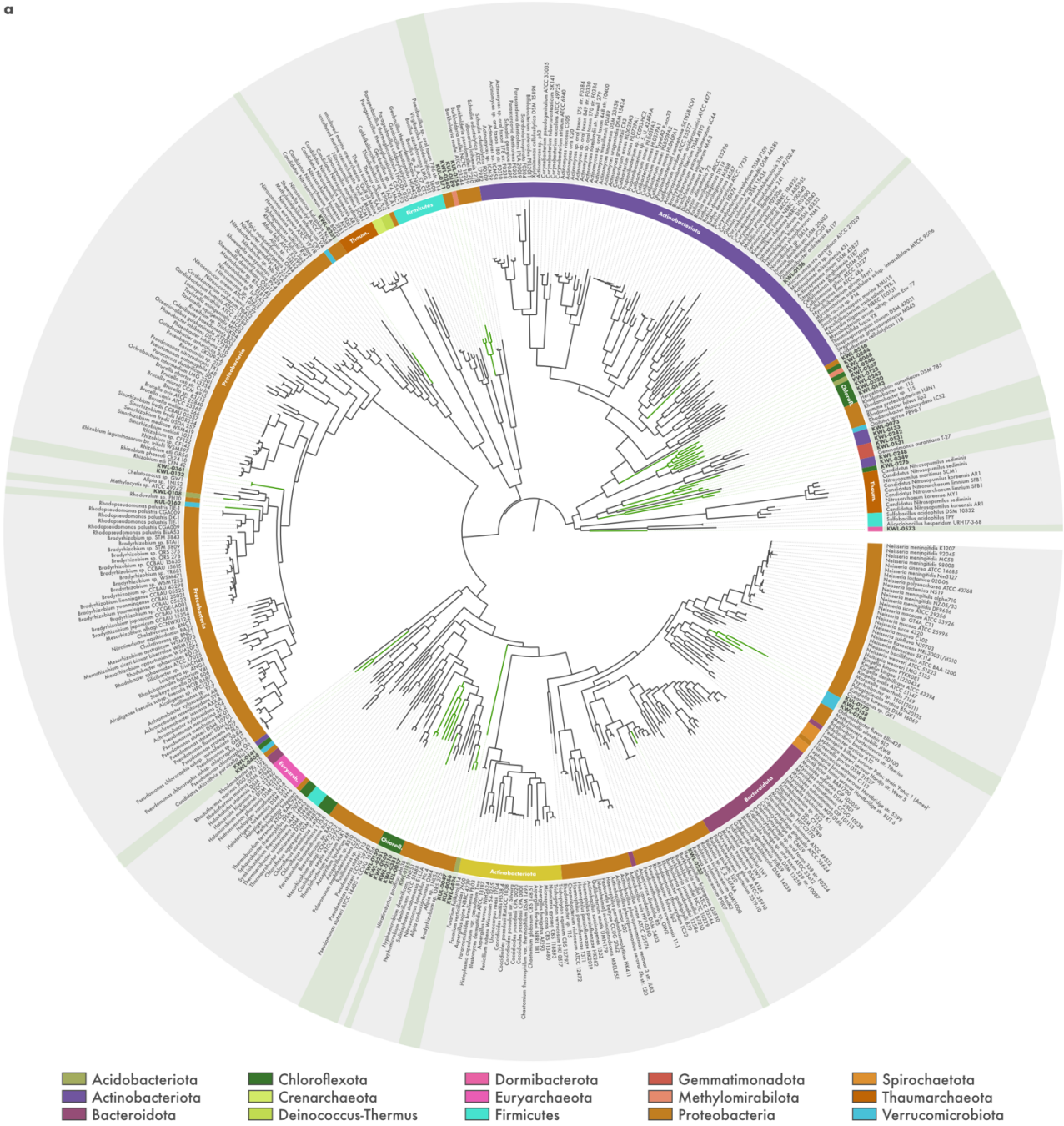

Suppl. Fig. S5 | Phylogeny of a) *nirK*, b) *nirS*, c) *norB*, and d) *nosZ* sequences from metagenome-assembled genomes (MAGs) recovered from tundra soils in Kilpisjärvi, northern Finland. Midpoint-rooted maximum-likelihood trees of translated sequences from Kilpisjärvi MAGs (highlighted) along with reference sequences from archaeal and bacterial genomes.

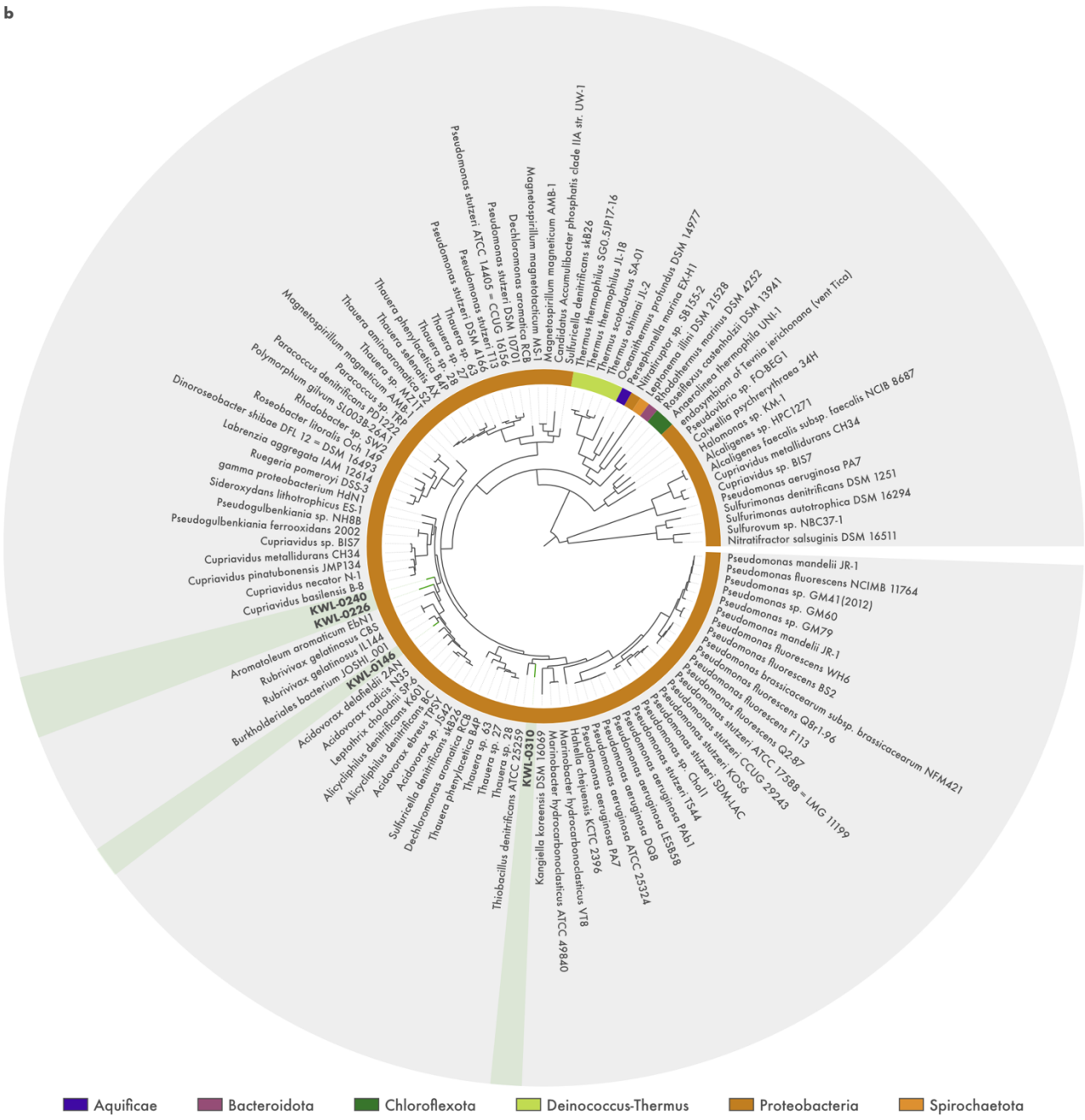
b
Candidatus Accumulibacter phosphatis clade IIA str. UW-1
Sulfuricella denitrificans skB26
Thermus thermophilus SG0.5JP17-16
Thermus thermophilus JL-18
Thermus scotoductus SA-01
Thermus ochrai JL-2
Oceanithermus profundus DSM 14977
Persephonella marina EX-H1
Nitratiruptor sp. SB155-2
Leptonema illini DSM 21528
Rhodothermus marinus DSM 4252
Roseiflexus castenholzii DSM 13941
Anaerolinea thermophila UNI-1
endosymbiont of Tevnia jerichonana (vent Tica)
Pseudovibrio sp. FO-BEG1
Colwellia psychrerythraea 34H
Alcaligenes faecalis subsp. faecalis NCIB 8687
Halomonas sp. KM-1
Alcaligenes sp. HPC1271
Cupriavidus metallidurans CH34
Cupriavidus sp. BIS7
Pseudomonas aeruginosa PA7
Pseudomonas denitrificans DSM 1251
Sulfurimonas autotrophica DSM 16294
Sulfurimonas denitrificans
Sulfurovum sp. NBC37-1
Nitratifractor salsuginis DSM 16511
Pseudomonas mandelii JR-1
Pseudomonas fluorescens NCIMB 11764
Pseudomonas sp. GM41(2012)
Pseudomonas sp. GM60
Pseudomonas sp. GM79
Pseudomonas mandelii JR-1
Pseudomonas fluorescens WH6
Pseudomonas fluorescens BS2
Pseudomonas brassicacearum subsp. brassicacearum NFM421
Pseudomonas fluorescens Q8r1-96
Pseudomonas fluorescens F113
Pseudomonas fluorescens Q2-87
Pseudomonas stutzeri ATCC 17588 = LMG 11199
Pseudomonas stutzeri CCUG 29243
Pseudomonas stutzeri KOS6
Pseudomonas stutzeri SDM.LAC
Pseudomonas sp. Ch01
Pseudomonas stutzeri TS44
Pseudomonas aeruginosa PAb1
Pseudomonas aeruginosa LESB58
Pseudomonas aeruginosa DG8
Pseudomonas aeruginosa ATCC 25324
Pseudomonas aeruginosa PA7
Pseudomonas aeruginosa KCTC 2396
Hahella chejuensis KCTC 2396
Marinobacter hydrocarbonoclasticus VT8
Marinobacter hydrocarbonoclasticus ATCC 49840
Magnetospirillum magneticum AMB-1
Magnetospirillum magnetotacticum MS-1
Magnetospirillum magnetotacticum RCB
Dechloromonas aromatica RCB
Pseudomonas stutzeri DSM 10701
Pseudomonas stutzeri T13
Pseudomonas stutzeri ATCC 14405 = CCUG 16156
Pseudomonas stutzeri DSM 4166
Pseudomonas stutzeri ATCC 17588
Thauera sp. 63
Thauera sp. 27
Thauera sp. 28
Thauera sp. 29
Thauera sp. 65
Thauera sp. 28
Thauera sp. 63
Thauera sp. 29
Thauera sp. 28
Thauera sp. 29
Thauera sp. 28
Thauera sp. 29
Thauera sp. 28

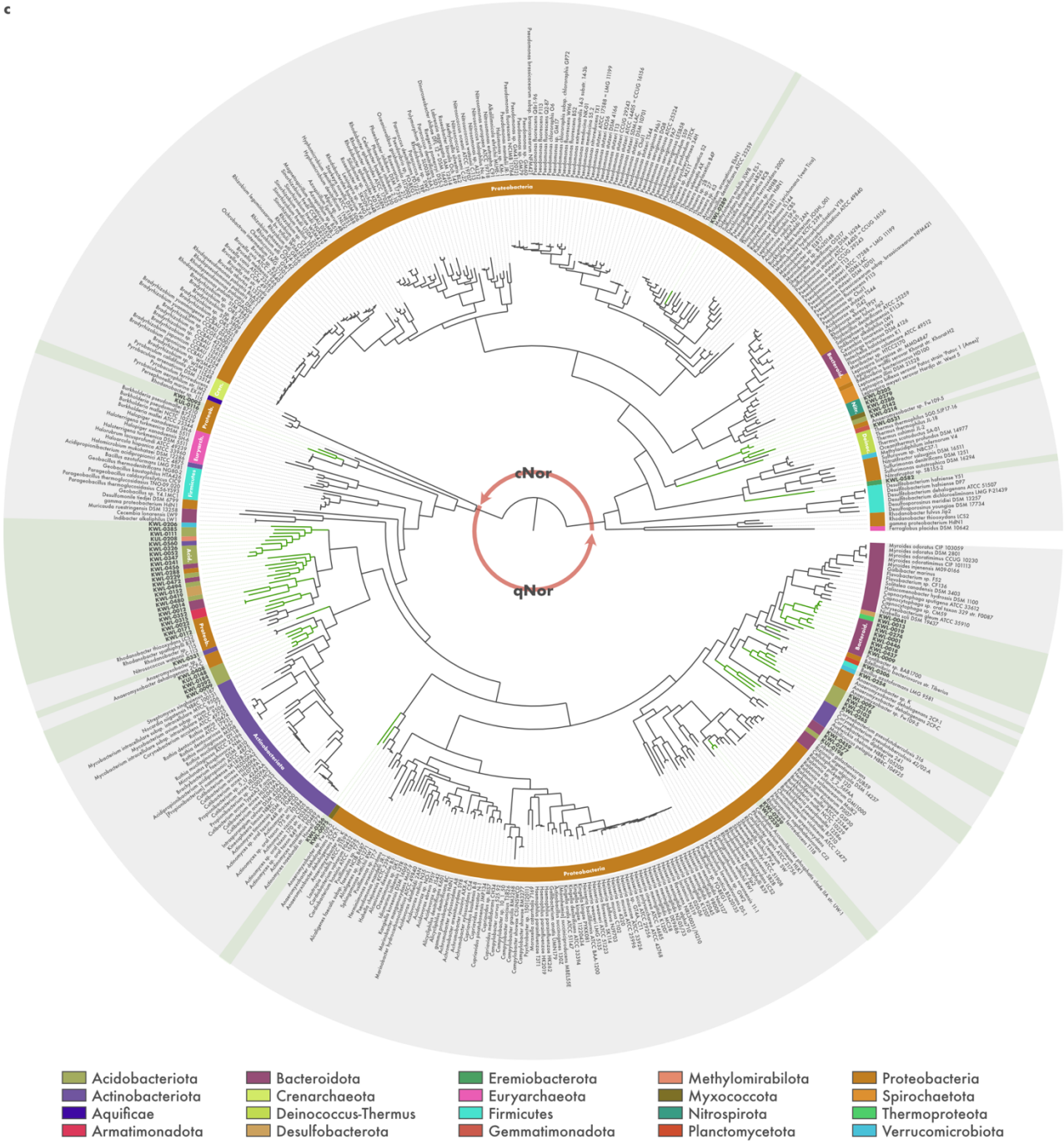

Suppl. Fig. S5 (continued) | Phylogeny of a) *nirK*, b) *nirS*, c) *norB*, and d) *nosZ* sequences from metagenome-assembled genomes (MAGs) recovered from tundra soils in Kilpisjärvi, northern Finland. Midpoint-rooted maximum-likelihood trees of translated sequences from Kilpisjärvi MAGs (highlighted) along with reference sequences from archaeal and bacterial genomes.

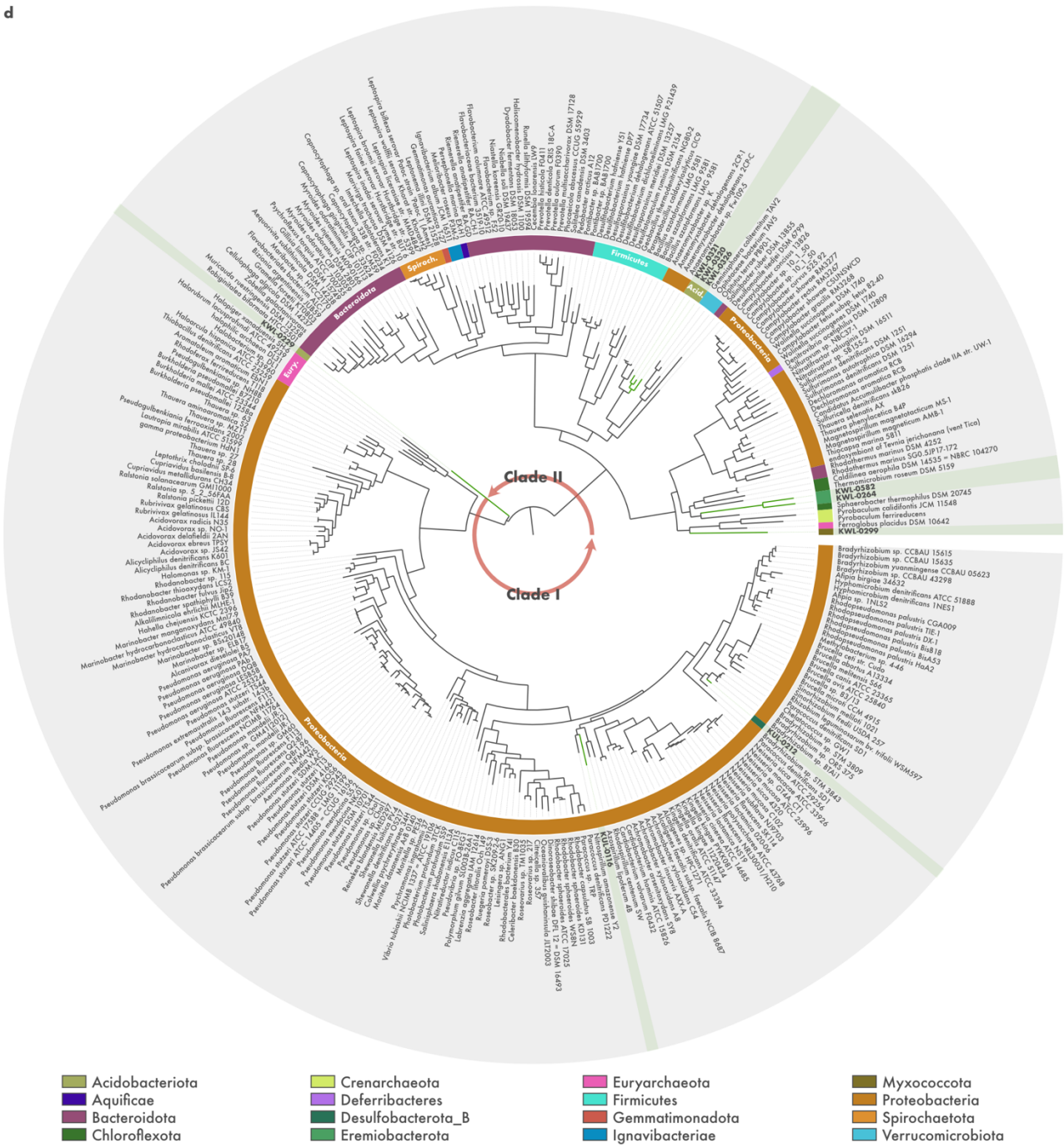

925 **Suppl. Fig. S5 (continued) | Phylogeny of a) *nirK*, b) *nirS*, c) *norB*, and d) *nosZ***
926 **sequences from metagenome-assembled genomes (MAGs) recovered from tundra**
927 **soils in Kilpisjärvi, northern Finland.** Midpoint-rooted maximum-likelihood trees of
928 translated sequences from Kilpisjärvi MAGs (highlighted) along with reference sequences from
929 archaeal and bacterial genomes.